Cape Peninsula
University of Technology

ENHANCED BIOSURFACTANT PRODUCTION BY *BACILLUS LICHENIFORMIS* STK 01 FOR HYDROCARBONS TARGETED FOR BIOREMEDIATION

By

CAROL ZETHU NGWENYA

Thesis submitted in fulfilment of the requirements for the degree

Magister Technologiae: Environmental Health

in the **Faculty of Applied Sciences**

at the

Cape Peninsula University of Technology

Supervisor: Prof. S.K.O. Ntwampe

Cape Town

2016

DECLARATION

I, *Carol Z. Ngwenya*, declare that the contents of this thesis represent my own unaided work, and that the thesis has not previously been submitted for academic examination towards any qualification. Furthermore, it represents my own opinions and not necessarily those of the Cape Peninsula University of Technology and the National Research Foundation of South Africa.

18-Aug-2016

Signed | Date

ABSTRACT

Environmental remediation of organic and inorganic contaminants such as hydrocarbons has been a research focus area of interest. Chemical surfactants have been extensively used for the remediation of contaminated sites for immobilisation of hydrocarbons from environmental matrices. The focus has been on the impact of chemical surfactants on the environment. These petroleum-based chemical surfactants have raised serious environmental concerns as: 1) they are toxic, 2) they deteriorate the environment owing to their non-biodegradability, 3) they are costly, and 4) most are not intended for environmental applications. As such, alternatives had to be found to mitigate concerns associated with the application of such synthetic surfactants in bioremediation.

Biosurfactants produced by microorganisms are a potential alternative to these synthetic surfactants. They have minimal environmental impact, are biodegradable and can withstand extreme conditions. However, biosurfactants are associated with high production costs and low production yield. Currently, large-scale production of biosurfactants cannot be achieved. Most research focuses on improving production yield which will contribute to the reduction in production costs. A lichenysin lipopeptide biosurfactant producing *Bacillus* sp., which grew exclusively on *Beta vulgaris* agrowaste, was identified. The microorganism was found to be an effective emulsifier for high molecular weight hydrocarbons such as, lubricant oil and diesel.

The aim of this study was to improve biosurfactant production yield from this *Bacillus* sp., including emulsification efficacy by optimising fermentation conditions by supplementing the broth with biocompatible nanoparticles synthesised using a green chemistry approach with *B. vulgaris (B. vulgaris)* extracts. This study also aimed at reducing production costs by using *B. vulgaris* agrowaste exclusively as the production medium, both for the biosurfactant and the nanoparticles.

Nanoparticles were synthesised using solely *B. vulgaris* plant extract as a metal precursor, reducing and capping agent. Nanoparticles were synthesised at slightly elevated temperatures (80 ˚C) and alkaline pH (8). The successfully produced nanoparticles were characterised using electron microscopes (TEM and SEM-EDS), spectrophotometric techniques (UV-vis and FTIR) as well as Power X-ray diffraction (PXRD). The synthesised nanoparticles were used to enhance biosurfactant production by *Bacillus licheniformis* STK 01. The crude biosurfactant was quantified using the gram dry weight method. Biosurfactant production was carried out under both aerobic and anaerobic conditions. The production was also assessed in fed-batch fermentations supplemented with produced nanoparticles at

specified time intervals. The fermentation parameters such as pH and redox potential were closely monitored during the course of fermentation.

Nanoparticle characterisation results revealed crystal spherical shaped Ca-based nanoparticles of approximately 10 nm size. Betanin found in *B. vulgaris* was largely responsible for the chemical reduction of metal ions to nanoparticles. At elevated temperatures, the Betanin releases an active hydrogen ion from the hydroxyl functional group. The dissociated proton binds and reduces metal ions in the solution into nanoparticles.

Furthermore, biosurfactant production was greatly enhanced using the biocompatible Ca-based nanoparticles. In fermentations in which *B. vulgaris* was the sole carbon source, the production yield was found to be 0.01 gdw/L and 0.03 gdw/L under aerobic and anaerobic conditions respectively. Furthermore, biosurfactant yield was enhanced in nanoparticle containing media for which the yield was increased to 0.05 gdw/L and 0.04 gdw/L under aerobic and anaerobic conditions respectively. However, fed-batch fermentations had the highest biosurfactant yield recorded, with biosurfactant yield of 0.35 gdw/L under aerobic conditions and 0.27 gdw/L under anaerobic conditions.

In a previous study, biosurfactant produced by the *Bacillus licheniformis* STK 01 using *B. vulgaris* exclusively had an emulsification index (E_{24}) of 20% for kerosene. However, by supplementing the biocompatible Ca-based nanoparticles in biosurfactant producing media by *Bacillus licheniformis* STK 01, improved the emulsification index of the produced biosurfactants to 50% using kerosene. This was an indication not only of the high production yield, but also of the emulsification activity of the lichenysin biosurfactant produced, including the influence of the biocompatible Ca-based nanoparticles used.

ACKNOWLEDGEMENTS

I wish to thank the following persons and instances:

- CPUT for the University Research Fund (RK16) used for the procurement of chemicals and resources required for this project to be a success.
- The National Research Foundation for financial support.
- My supervisor, Prof. S.K.O. Ntwampe, for his assistance, guidance and technical input.
- Biotechnology laboratory staff for allowing me to use their resources.
- The Department of Biotechnology staff for their input.
- Bioresource Engineering Research Group (*BioERG*) members for their technical support.
- Lukhanyo Mekuto, Notemba Silwana and Margaret Mazyambe for their moral and technical support. I am truly grateful.
- My supportive siblings, Precious Mazibuko and Mthobisi Ngwenya, and my loving grandmother, Fikile Mazibuko, for their love and support.
- My spiritual parents, Pastor Bongane Msibi and Pastor Lindiwe Msibi for spiritual guidance, support and constant prayers. Thank you for not giving up on me.
- My wonderful friends, Pretty Nkuna, Mzikazi Fuzile, Nela Shikimeni, Tshepo Motene and Charlene Mabotja for helping me believe in myself.
- The University of Cape Town Electron Microscope Unit (EMU), The University of Western Cape Electron Microscope Unit, and Stellenbosch University Central Analytical Facility, for providing access to their equipment.

DEDICATION

To my late mother, L. Mazibuko and Grandfather T.J. Mazibuko

Your memories have been a source of inspiration.

TABLE OF CONTENTS

LIST OF FIGURES

LIST OF TABLES

GLOSSARY

Terms/Acronyms/Abbreviations	Description
A. vera	*Aloe vera*
Acetyl-CoA	Acetyl coenzyme A
Asp	Aspartic acid
ATP	Adenosine triphosphate
B. vulgaris	*Beta vulgaris*
BOD	Biochemical oxygen demand
BXYL	Xylosidase
COD	Chemical oxygen demand
CTAB	Cetyltrimethylammonium bromide
DNA	Deoxyribonucleic nucleic acid
DO	Dissolved oxygen
DWAF	Department of Water Affairs and Forestry
EDS	Energy dispersive spectroscopy
FTIR	Fourier transform infrared spectroscopy
GC	Guanine & Cytosine
Gdw/L	Gram dry weight per litre
Gln	Glutamine
Glu	Glutamic acid
HMW	High molecular weight
HPLC	High performance liquid chromatograph
ICP-MS	Inductively coupled plasma mass
Ile	Isoleucine
Lch	Lichenysin
Leu	Leucine
LMW	Low molecular weight
M1	Medium 1
M2	Medium 2
M3	Medium 3
M4	Medium 4
M5	Medium 5
ORF	Open reading frame
PheA	Phenylalanine
RNA	Ribonucleic acid
rRNA	Ribosomal ribonucleic acid
SEM	Scanning electron microscope
SSF	Solid state fermentation
TEM	Transmission electron microscope
TISAB	Total ionic strength adjustment buffer
Try A	Tyrosine
UV-Vis	Ultra violet-visible light
Val	Valine
X-Ray	X-radiation
αAGLU	Alpha-Galactosidase
βGAL	Beta-Galactosid

CHAPTER 1
INTRODUCTION

1.1 Background

Biosurfactants are produced by a variety of microorganisms including bacteria, yeast and fungi. They are secreted extracellularly (Desai & Banat, 1997). They are surface-active agents that reduce interfacial tension between immiscible liquids enabling them to mix (Marchant & Banat, 2012). They are amphiphilic molecules with a hydrophilic (typically a hydrocarbon chain) and a hydrophobic region (chain of fatty acids) that vary depending on the producing organism. The hydrophilic and hydrophobic moieties interact with the phase boundary in a heterogeneous system to reduce the surface tension (Fracchia et al., 2012). They have unique physiochemical properties (Reis et al., 2013) which broaden their application in many different fields. They can be used as food additives, in cosmetics (including detergent formulation), as well as in combination with other enzymes for wastewater treatment. They also have the potential to replace chemical surfactants in industrial processes for lubrication, wetting, foaming, softening, fixing dyes, stabilising dispersions, as well as in bioremediation processes (Reis et al., 2013).

The widespread use of biosurfactants is limited, owing to the low production yields and high production cost. Factors that contribute to high production cost are mainly the use of refined nutrients that the microorganisms utilise for growth and subsequent production of the biosurfactant. Agrowaste materials have been used as substrates for the production of biosurfactants in an attempt to reduce costs (Kiran et al., 2011). To ensure optimal growth and high production yields, agrowaste materials are still supplemented with commercial growth media thus increasing production costs. It is through research that highly efficient biosurfactant-producing microorganisms can be engineered and used in the design of fermentation processes in which the use of unconventional substrates can be explored, thus reducing the production costs of biosurfactants (Burgos-Díaz et al., 2012).

Bacillus licheniformis STK01 was shown to grow on different agrowaste such as *B. vulgaris* agrowaste, while producing biosurfactants with a high surface activity; results which are comparable with those reported when refined substrates were used (Amodu et al., 2014).

In an attempt to improve biosurfactant production yield, nanoparticles have also been employed to enhance biosurfactant production. Glycolipids production by *Nocardiopsis* sp. MSA13A was increased by 80% in a solid state culture supplemented with iron (Fe) nanoparticles (Kiran et al., 2014). There have been reports suggesting that different nanoparticles have a great influence on microbial growth and subsequent production of secondary metabolites (Flores et al., 2004; Liu et al., 2013).

Additionally, it was hypothesised that trace metal availability is one of the critical factors for enhanced biosurfactant production (Kiran et al., 2014). However, the production processes of these nanoparticles used to enhance biosurfactant production are considered environmentally unfriendly and thus their use will have significant negative environmental impact.

In a study by Kiran et al. (2014), nanoparticles were synthesised using the foam method with cationic CTAB surfactant as a reducing agent and $NaBH_4$ as a stabiliser. These synthetic chemicals introduce pollutants into the environment and pose health risks. However, there has been development in the methods used for the synthesis of nanoparticles by employing environmentally friendly and non-toxic processes termed the 'green synthesis of nanoparticles' (Malik et al., 2014). This includes the use of biological materials such as microorganisms, and their secondary metabolites, plant extracts, as well as agrowaste. In a study carried out by Gan et al. (2012), palm oil mill effluent was used as a reducing and stabilising agent for the synthesis of Au nanoparticles from a chloroauric acid solution ($HAuCl_4$), which was a source of a metal precursor. However, this procedure produced chemical waste from the source of the precursor used. Le et al. (2013) also produced silica (Si) nanoparticles from Vietnamese rice husk which was used as a source of a metal precursor but used analytical grade synthetic chemicals as reducing and stabilising agents. The waste from such processes also contributes to environmental pollution.

1.2 Problem statement

Petroleum-based chemical surfactants pose a major threat to the environment, as these compounds often lead to contamination of soil and water sources, thus contributing to environmental health-related complications. Currently, processes used for the remediation of hydrocarbon-contaminated sites have been proved to be capital intensive. Chemical surfactants have been used throughout the world for the recovery of hydrocarbons for a variety of purposes. These chemical surfactants have raised environmental concerns, as they are toxic and in certain cases are non-biodegradable.

There is thus a need for the development and production of surfactants that are environmentally friendly by using economically feasible processes with lower costs. Biosurfactants are a potential alternative to these chemical surfactants, as they have a low environmental impact, are biodegradable, and can withstand extreme conditions. However, the major impediment to using biosurfactants is high production costs and low production yield. As a result, large-scale production cannot be achieved at present.

1.3 Hypothesis

Optimisation of the fermentation process using biocompatible nanoparticles as a supplementary support additive would increase biosurfactant yields, including emulsification activity.

1.4 Research objectives

This study had two aims. The first aim of was to develop a method for the green synthesis of metallic nanoparticles using *B. vulgaris* agrowaste solely, to provide a completely green and environmentally benign method for nanoparticles synthesis. The second aim was to supplement the metallic nanoparticles in the production media to enhance biosurfactant production by *Bacillus licheniformis* STK 01, a microorganism previously shown to produce biosurfactant with a high emulsification activity.

Aim 1:
Synthesis of biocompatible metallic nanoparticles from *B. vulgaris* agrowaste using a completely green chemistry approach.

Objectives:

- Optimisation of production conditions for the green synthesis of the biocompatible nanoparticles.
- Determination of an ideal *B. vulgaris* solution and concentration for the synthesis of nanoparticles.
- Purification and recovery of the synthesised nanoparticles.
- Subsequent characterisation of the produced nanoparticles using powder X-ray diffraction, spectroscopic and electron microscopic techniques.

Aim 2:
To enhance biosurfactant production by *Bacillus licheniformis* STK 01 using the biocompatible nanoparticles for improved emulsification activity.

Objectives:

- Perform biochemical analyses on the bacterium used for the production of the biosurfactant.
- Enhance biosurfactant production using biocompatible nanoparticles under both aerobic and anaerobic conditions.
- Monitor fermentation parameters such as dissolved oxygen (DO), pH and redox potential, in a growth medium primarily containing the *B. vulgaris* agrowaste without synthetic nutrient media supplementation.
- Recover and quantify the biosurfactant yield.
- Investigate biosurfactant activity by emulsification of a hydrocarbon previously found to be difficult to emulsify.

1.5 Significance of the study

The attributes of enhanced biosurfactant production by the strain used, by utilising agrowaste material, can be further developed for industrial applications, through bioremediation of contaminants such as hydrocarbons produced from petroleum and related industries. This will improve yields on a large scale, while reducing production costs.

1.6 Delineation of the study

This project did not cover the following:

- Utilisation of other agrowaste material by *Bacillus licheniformis* STK 01, as this was previously done by Amodu et al. (2014).
- Applications of the biosurfactant in situ, that is, in field studies.
- Characterisation of the biosurfactant produced.

CHAPTER 2
LITERATURE REVIEW

2.1 Use of chemical surfactants in environmental bioremediation

Environmental pollution is a global concern increasing annually, causing irreparable damage to the overall health of the environment. There are various sources of environmental pollution: one that poses environmental deterioration is the improper disposal of waste generated by manufacturing industries. A study conducted by the Dolphin Coast landfill management (KwaZulu-Natal) reported over 42 million m^3 of general waste generated every year, with the Gauteng province being the largest contributor, followed by Mpumalanga and KwaZulu-Natal, owing to mining and agricultural activities in these two provinces. Additionally, 5 million m^3 of hazardous waste is produced annually from mining activities, including the production of fertilisers. According to Nkosi (2014), mining is reportedly the biggest contributor of hazardous waste, accounting for 72.3% of the total hazardous waste generated, followed by pulverised fly ash (6.7%), agricultural waste (6.1%), urban waste (4.5%) and sewage sludge (3.6%).

Furthermore, waste can be classified into two categories: general waste and hazardous waste. General waste is waste that is not harmful to the environment and that poses minimal environmental health-related issues, although it contributes to environmental degradation. On the other hand, hazardous waste is waste that contains hazardous organic and inorganic compounds that have an adverse impact on human, animal and environmental health (Bredenhann, 1998). Hazardous waste material that is improperly disposed of into the environment is difficult to remediate. It requires extensive treatment with capital-intensive equipment and the use of other chemical-based solutions that further contribute to environmental pollution. The chemical compounds used to facilitate treatment for such waste include alcohols, ethers, ketones, aromatics, straight chain alkanes and petroleum products. Another example of chemical-based waste treatment processes is waste solidification, which involves solidifying the contaminants to enhance their removal. This involves removing moisture, by using absorbents such as grounded clay, followed by polymerisation with chemical reagents. In certain instances this process includes freeze drying (Wuana & Okieimen, 2011).

The most commonly used treatment agents produced and used in large quantities are chemical surfactants. These are considered as surface tension reducing compounds. They reduce adhesion forces between contaminants and the carrier matrices, augmenting physical cleaning methods and increasing the mobility of the contaminants for treatment (Farn, 2006). What must be taken into consideration is that such surfactants are produced from petroleum or oleochemical-based sources developed for large-scale industrial applications and in most instances these surfactants are non-biodegradable. These types of surfactants are produced in various forms; they can either be in ionic and non-ionic forms, with cationic surfactants being the most toxic and anionic surfactants less toxic (Burgos-Díaz et al., 2012).

These treatment agents have been successfully used to enhance remediation of hazardous contaminants in environmental matrices (Mulligan et al., 2001). However, their toxicity raises additional contamination problems, a focus research area for environmentalists. Upon remediation of the environment, the surfactants' residue remains in the environment, posing persistent environmental health issues and becoming a threat to aquatic life, among others. This is due to surface activity that may interfere with the biological membrane processes of organisms and facilitate foreign toxic substances into the cells of organisms. Unfortunately, some are non-biodegradable, therefore cannot be degraded directly by using biocatalysts or any other biological means. Furthermore, in most instances, chemical surfactants are produced from non-renewable resources on a large scale by using processes that contribute to the deterioration of ecosystems, thus wasting useful resources (Burgos-Díaz et al., 2012).

Awareness of the use of renewable-based products has resulted in the urgent need for the development of alternatives for chemical surfactants. Consequently, the exploration of biosurfactant utilisation has received considerable attention. Biosurfactants are microbial surfactants produced by microorganisms in fermentation processes, using carbon sources such as reducible sugars, vegetable oils and agricultural waste (Banat et al., 2014). Intriguingly, these biological surfactants have minimal adverse environmental impact and have been proved to be suitable alternatives with numerous advantages over chemical surfactants (Marchant & Banat, 2012). It has also been discovered that they can withstand extreme conditions such as high temperature, high salinity and low pH, making them applicable in a variety of environmental conditions. However, low production yields and high production costs due to the use of expensive refined substrates limit their use (Makkar & Cameotra, 2002), although costs can be minimised by using low-cost substrates and improving fermentation conditions to enhance the yield.

To increase the competitiveness of biosurfactant usage in comparison with chemical surfactants, it is indispensable to focus on cost, functionality and production capacity; thereby improving other factors that can be considered important in biosurfactant production. In an attempt to improve production capacity, including yields, highly efficient microorganisms can be used. Production can be enhanced by the manipulation of biosurfactant coding genes (Sekhon et al., 2011), although genetically modified organisms are only applicable under strict laboratory conditions and are not suitable for environmental applications. Furthermore, improving fermentation conditions has been shown to improve production capacity. Kiran et al. (2014) proposed that supplementing nanoparticles in a bioprocess for biosurfactant production reduces the impact of non-metallic ions of mineral salts generally used in the media, while improving production yields.

However, the methods employed for the synthesis of the nanoparticles required to improve biosurfactant production yields is characterised by high temperatures and pressures, and energy-intensive requirements, while the process uses highly toxic chemicals (Makarov et al., 2014) which defile the purpose of green chemistry synthesis and environmental conservation.

The new emerging field of nanobiotechnology provides possible innovative solutions for improving bioprocess conditions by the direct application of nano-materials. To further reduce production cost, inexpensive microbial growth substrates are utilised, reducing the production cost by 10 to 30% compared with using refined substrates. Current research on the selection of a suitable substrate has centred on agricultural waste, that is, agrowaste (Banat et al., 2014). The use of agrowaste minimises cost associated with treatment and disposal of the waste, and synergistically provides a solution to the issue of environmental pollution (Burgos-Díaz et al., 2012).

2.2 Biosurfactants: alternatives to synthetic surfactants

Biosurfactants are unique compounds of biological origin with vast applications in many fields (Amodu et al., 2014). Their structural diversity is determined by the producing organism, raw material used and processing conditions (Burgos-Díaz et al., 2012). They are amphiphilic molecules consisting of a hydrophilic moiety, comprising an acid, peptide, cation, anion, mono- or di-polysaccharide and a hydrophobic moiety which can either be saturated or unsaturated hydrocarbon chains or fatty acids (Saharan et al., 2012).

2.2.1 Classification of biosurfactants

Biosurfactants are classified according to their chemical structure and microbial origin. Microbial origin classification depends on the type of producing microorganism and the functional groups in the surfactant. Microorganisms such as bacteria, fungi and yeast produce different biosurfactants. Structural classifications of biosurfactants fall largely in two categories: Low Molecular Weight (LMW) and High Molecular Weight (HMW) biosurfactants.

LMW biosurfactants include glycolipids and lipopeptides (Fracchia et al., 2012). HMW biosurfactants include bioemulsifiers, which are divided into lipoproteins, protein polysaccharides and lipopolysacharides. The latter are grouped together as polymeric biosurfactants (Fracchia et al., 2012); unlike LMW biosurfactants, they do not lower the surface tension of liquids but rather stabilise emulsions. Overall, LMW biosurfactants efficiently reduce surface and interfacial tension. Examples include glycolipids and lipopeptides. A well-studied glycolipid is the rhamnolipid produced by *Pseudomonas aeruginosa* (Reis et al., 2013; Zhao et al., 2014; Bhardwaj et al., 2015). Where lipopeptides are concerned, surfactin is a well-studied biosurfactant produced by *Bacillus subtilis*, which exhibits high surfactant activity properties. On the other hand, a biosurfactant similar to Surfactin synthesised by *Bacillus licheniformis*, a LMW lipopeptide termed 'lichenysin', was reported to be more efficient than the LMW lipopeptide surfactin (Grangemard et al., 1999). Additionally, Joshi et al. (2013) isolated biosurfactant-producing organisms from a diversified habitat which were determined to be similar to those produced by *Bacillus subtilis* and *Bacillus licheniformis*. The species were able to reduce the surface tension of water from 72 to 28 mNm^{-1}. Table 2.1 lists several biosurfactants produced using unconventional substrates for bioremediation purposes.

Table 2.1: Biosurfactants produced using unconventional substrates for bioremediation purposes

Biosurfactant	Class	Producing organism	Carbon source	Isolated environment	Environmental applications	Reference
Mannosylerythritol lipids	Glycolipid (LMW)	*Pseudozyma antarctica* PYCC 5048T *Pseudozyma aphidis* PYCC 5535T	Cellulostic material	Olive mill waste water	Petroleum biodegradation Bioconvension of chemical waste Enhanced bioremediation	Farias et al. (2014), Yu et al. (2015)
Rhamnolipid	Glycolipid (LMW)	*Pseudomonas aeruginosa* NCIM-2036	Wheat straw	Hydrocarbon-contaminated soil	Crude oil bioremediation and oil recovery	Prabu et al. (2015)
Sophorolipids	Glycolipids (LMW)	*Starmerella bombicola* (ATCC 22214)	Waste cooking oil	Honey of a bumblebee	Bioremediation	Maddikeri et al. (2015), Van Bogaert et al. (2007),
Trehalose Novel	Glycolipids (LMW) Lipopeptide (LMW)	*Rhodococcus* sp. PML026 *Bacillus siamensis* RT10	Sunflower oil Crude oil	Seawater Oil-soaked soil	Hydrocarbon bioremediation Environmental remediation	White et al. (2013), Franzetti et al. (2010) Varadavenkatesan & Murty (2013)
Novel	Lipopeptide (LMW)	*Staphylococcus* sp. strain 1E	Olive oil	Crude oil contaminated soil	Bioremediation	Eddouaouda et al. (2012)
Lichenysin	Lipopeptide (LMW)	*Bacillus licheniformis* STK01	*B. vulgaris*	Rotting wood	Heavy carbon recovery	Amodu et al. (2013), Joshi et al. (2015)
Surfactin	Lipopeptide (LMW)	*Bacillus subtilis* #573	Corn Steep liquor	Crude oil	Enhanced oil recovery	Gudiña et al. (2015)

2.2.2 Lichenysin biosurfactant

Lichenysin is a type of biosurfactant produced mainly by *Bacillus licheniformis* specie (Joshi et al., 2015). It is an amphiphilic anionic microbial surfactant. Nerurkar's (2010) views suggest that structural and molecular analysis of lichenysin lipopeptide biosurfactants reveal that each lipopeptide molecule is made up of a lipid moiety of fatty acid constituting the hydrophobic moiety and seven amino acids comprising the hydrophilic moiety (Figure 2-1).

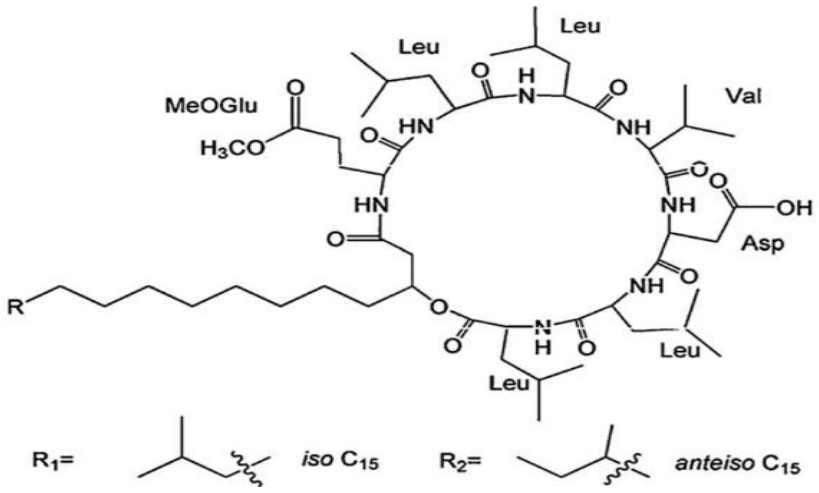

Figure 2-1: **Molecular structure of lichenysin biosurfactant**

There are five types of lichenysin, namely, lichenysin A, B, C, D and G. They differ on the basis of their amino acid peptide primary structure (see Table 2.2).

Table 2.2: Types of lichenysin biosurfactants

Biosurfactant	Peptide Structure						
Lichenysin A	L-Gln	L-Leu	D-Leu	L-Val	L-Asp	D-Leu	L-Ile
Lichenysin B	L-Glu	L-Leu	D-Leu	L-Val	L-Asp	D-Leu	L-Leu
Lichenysin C	L-Glu	L-Leu	d-Leu	L-Val	L-Asp	D-Leu	L-Ile
Lichenysin D	L-Gln	L-Leu	D-Leu	L-Val	L-Asp	d-Leu	L-Ile L-Leu L-Val
Lichenysin G	L-Gln	L-leu L-Ile	D-Leu	L-Val L-Ile	L-Asp	D-Leu	L-Ile L-Val
Surfactin	L-Glu	D-Leu	D-Leu	L-Val	L-Asp	D-Leu	L-Leu

The chemical structure of lichenysin is similar to that of surfactin, except for variations on the first amino acid group in lichenysin A, D and G. These amino acids have an L-Gln instead of an L-Glu. However, Lichenysin B and C have L-Glu similar to surfactin on the first position. Additional similarities are observed on position 2 to 6, except that for lichenysin G, the second and fourth amino acid groups' variations depend on the nitrogen source available in the production media. Desai and Banat (1997) determined that the second amino acid group, that is, L-leu or L-val on surfactin, could be influenced by L-amino acid concentrations in the nutrient medium. Therefore, the nitrogen source in the production medium also determines the seventh amino acid group for lichenysin G and D. It can either be L-lle, L-val for lichenysin G and L-Leu for lichenysin D. Lichenysin A exhibits what is referred to as the general primary structure of lichenysin. Lichenysin B is structurally identical to surfactin at the peptide portion and only differs in the lipid tail. The β-hydroxy fatty acid of lichenysin B contains an average of 8 to 9 methylene group of isoforms, whereas lichenysin C contains four distinct fatty acid chains. Additionally, lichenysin A is a mixture of 14 β-hydroxy fatty acids (Nerurkar, 2010).

2.2.3 Biosynthesis of lichenysin

The amphiphilic structure of lichenysin biosurfactant is synthesised using two different metabolic pathways: one for the synthesis of the hydrophobic (fatty acids) and the other for the hydrophilic (amino acids) moieties. Under normal conditions the pathways utilise a common precursor. However, each pathway utilises a different set of enzymes. Similarities between the two pathways have been observed with the first set of enzymes used to catalyse the precursor enzymes, which can be classified as regulatory enzymes. It should be noted that both pathways are substrate dependent. The two moieties are synthesised *de novo*. The hydrophobic moiety is substrate induced, while the synthesis of hydrophilic moiety is substrate dependent (Desai & Banat, 1997), which therefore determines the components of the hydrophilic moiety.

Biosurfactant synthesis is regulated by quorum sensing, a microbial gene regulation technique dependent on cell density to express specific enzymes (Das et al., 2008). Mechanisms involved in gene regulation include induction and repression (Desai & Banat, 1997). LMW signal molecules have been reported to induce biosurfactant production (Das et al., 2008). Additionally, induction controls the onset of biosurfactant synthesis of most lipopeptide biosurfactants. However, organic acids and D-glucose have been reported to repress the production of biosurfactants by *Acinetobacter calcoaceticus* and *Arthrobacter paraffineus,* with a similar observation in rhamnolipid production by *Pseudomonas aeruginosa* (Desai & Banat, 1997). Other hydrocarbons and carbohydrates can be used as precursors of biosurfactant synthesis.

The carbon precursor enters the carbohydrate metabolism pathway, termed glycolysis, which starts with the catabolism of glucose for the production of energy in the form of ATP. In this pathway one molecule of glucose is converted into two molecules of key intermediates called pyruvate with several fates. Thereafter, some amino acids are produced from the pyruvate, followed by the conversion to acetyl-CoA, which serves as a starting material for the biosynthesis of fatty acids, a major component of lichenysin. The acetyl-CoA also enters the citric acid cycle as a precursor to the biosynthesis of several amino acids that make up the amino acid peptide of the lipopeptides, that is, lichenysin and other important biomolecules. Thereafter, the components of lichenysin, that is, amino and fatty acids, are processed by lichenysin synthetases coded in the lichenysin operon for the non-ribosomal synthesis of lichenysin biosurfactant (Desai & Banat, 1997; Konz et al., 1999; Roongsawang et al., 2010).

The multi-enzymes acting as independent enzymes with specific linkages that form the protein template facilitate the primary structure of the lichenysin peptide (Figure 2-2). The lichenysin synthetase transfers β-hydroxy fatty acids from the first acyltransferase module in lichenysin A synthetase, forming a hydroxyacyl amino acid that serves as the first intermediate of the reaction. The first six amino acids of the peptide for hydrophilic moiety are added by lch AA and lch AB while the last amino acid is added by lch AC. The activation site of the thioeterase protein is located at the C-terminal site of the lch AC product. Specific activation requires the β-hydroxy fatty acids and side chain of the fifth aspartate and seventh isoleucine to harbour specific pockets for binding of amino acid substrates, depending on the amino acid sequence of the peptide. lch AA1, lch AB2 and lch AC activate Gln, Asp and Lle with a high degree of substrate specificity. Therefore, the A domain recognises and activates the amino acids while the C-domain joins the two adjacent amino acid molecules for peptide bond formation depending on the structure of the donor, including the acceptor amino acid (Nerurkar, 2010). The operon of the biosurfactant of interest for this study, lichenysin, is shown in Figure 2-2.

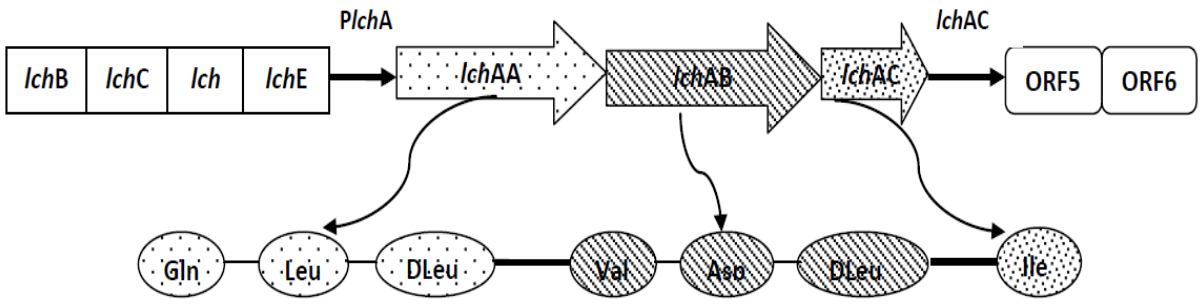

Figure 2-2: The lichenysin operon

2.3 Bioprocess condition for the production of biosurfactants

The most suitable type of fermentation process for production of biosurfactants is Solid State Fermentation (SSF). This is influenced by the organism's ability to grow on different solid matrices (Soberón-Chávez, 2011). Microorganisms in SSF are grown on moist solid particles. Surrounding the solid particles is adsorbed water that forms a thin film, making the particles moist, so that cells can adhere efficiently to form biofilms. In between the solid particles and immobilised organisms exists a continuous gas phase. The requirements of an effective SSF include that a pure culture, or several pure cultures, be inoculated at once or at different time intervals. The most suitable microorganisms to use in an SSF are filamentous fungi; however, bacteria and yeast have also been employed (Mitchell et al., 2006).

For example, rhamnolipid production was observed to increase ten-fold for *Pseudomonas aeruginosa* UFPEDA 614 grown on a solid carrier in an SSF (Camilios-Neto et al., 2011). Substrates often used for SSF include residues of agricultural produce, forestry and food-processing waste. These by-products contain polymers that are part of the solid particles matrix making the particles structurally solid.

2.3.1 Influence of temperature and dissolved oxygen

Although during SSF unfavourable environmental conditions may occur, there is a need to closely monitor the fermentation as reduced microbial growth can take place, thus reducing biosurfactant production. Temperature may vary during the organisms' growth cycle owing to metabolic activity which can result in its increase, reaching levels above the microorganisms' optimum growth temperature (Mitchell et al., 2006). Nevertheless, temperature can be controlled by exposing the microorganisms to a constant temperature throughout its growth cycle in the fermentation process (Pohlscheidt et al., 2013), by using temperature-controlling apparatus.

Additionally, oxygen supply is also limited in SSF especially in the deeper portions of the attached biomass (within the biofilm). However, if a significant quantity of dissolved oxygen is available on the surface of the solid matrix (Mitchell et al., 2006), this should be sufficient to meet immobilised microbial requirements. Dissolved oxygen is one of the most important parameters to control in bioprocesses as it influences culture performance. Dissolved oxygen (DO) has an impact on product quality, nutrient metabolism and cell culture performance, that is, yield. To monitor oxygen in the bacterial culture, DO needs to be constantly measured in situ by using dissolved oxygen probes. Temperature and dissolved oxygen requirements for biosurfactant production are inter-dependent and therefore can influence the performance of the biosurfactant-producing organism used in the fermentation.

Bacillus subtilis was observed to have had increased yields of lipopeptide biosurfactant under aerated conditions at 37 ˚C (Ghribi & Ellouze-Chaabouni, 2011). Similarly, rhamnolipid was produced under anaerobic conditions at 42 ˚C by a *Pseudomonas aeruginosa* strain (Zhao et al., 2014). This suggests that different fermentation conditions can be used to achieve similar fermentation outcomes.

2.3.2 Influence of pH and redox potential

Another difficult parameter to control during SSF is the pH. It was determined to have the greatest effect on the surface-active properties of the biosurfactant produced by *Lactobacillus pentoses* (Vecino Bello et al., 2012). The pH can also be monitored in situ using specialised pH probes. pH sensors used in fermentation depend on electrode design and functionality (Pohlscheidt et al., 2013). The pH electrode is linked to a redox sensor that measures the redox potential in millivolts (mV). Monitoring redox potential in fermentation media provides information on redox reactions in the fermentation and equilibrium state. During bioprocessing, the redox potential in the media vary over time owing to the constantly changing equilibrium of oxidising and reducing components which are a result of secreted proteins and other components by the bacterium. The redox potential is inversely proportional to the pH of the media as a result of chemical reactions of the media components (Pohlscheidt et al., 2013). Limited research has been conducted on the influence of redox potential for the production of biosurfactant in cultures, more especially for lichenysin production.

2.3.3 Growth-limiting nutrient media source influences

Nutrient depletion in fermentation media varies with biomass increase as microorganisms utilise nutrients for growth. In SSF, the nutrients are saturated within the solid particles; however, nutrient supply to the organisms may be limited (Mitchell et al., 2006). Nutrients such as carbon sources can decrease in concentration during the microbial growth cycle and can be quantified by the extraction of the residual carbon source in the fermentation broth subsequent to the determination of the concentration by using various analytical instruments such as gas chromatography or high-pressure liquid chromatography and spectrophotometric tests. The most applicable method for quantification of residual carbon source molecules is the dinitrosalicylic acid method proposed by Miller (1959), which is used for the estimation of total reducible sugars. This method can be used to estimate the quantity of fermentable sugars released from hydrocarbons used for biosurfactant production. For growth-influencing nutrients such as the nitrogen source and trace element requirements, see Section 2.3.4.

2.3.4 Nutritional requirements for biosurfactant production

Microorganism biomass consists of 50% carbon on a dry weight basis (Vogel & Todaro, 1997). The carbon source is the main requirement for biomass production. The carbon source is consumed through an energy-production pathway and produces CO_2 and other organic compounds, including lipopeptide biosurfactants' precursors, amino and fatty acids. In most cases, carbohydrates are the most commonly used carbon sources that are added in the media in concentrations higher than the other nutrients. According to Banat (1995), when a readily available carbon source is present in growth media, biosurfactant production decreases and increases when the carbon source is depleted. In a recent study conducted by Coronel-León et al. (2015) which assessed suitable carbon sources for the production of biosurfactant by *Bacillus licheniformis* AL1.1, high biosurfactant yield was reported using refined carbohydrates while minimal biomass growth and biosurfactant production were observed when oil was used. However, olive oil was determined to be the suitable carbon source for biosurfactant production by *Staphylococcus* sp. strain 1E (Eddouaouda et al., 2012). Therefore, carbon source selection for biosurfactant production is dependent on the microorganism's ability to utilise or degrade the available carbon source.

As previously explained, carbohydrates are catabolised more efficiently during glycolysis for the production of lipopeptide biosurfactant precursors, that is, amino and fatty acids. Amino acid subsequently induces the lichenysin operon (see Figure 2-2) for the non-ribosomal synthesis of lipopeptides (Nerurkar, 2010). Whereas with complex hydrocarbons such as oils, prior catabolisis is required to initially hydrolyse the hydrocarbons to their carbohydrate monomers utilising a specific set of enzymes. Therefore, high yields of biosurfactants can be obtained by using easily metabolisable carbohydrates as a carbon source. However, increased biosurfactant activity is favoured by using hydrocarbons that the microorganisms can readily utilise to reduce the surface tension between the immiscible liquid and the hydrocarbon. *Bacillus licheniformis* R2 and STK 01 grown on glucose and cellulosic material, respectively, reduced surface tension of the medium to 28 mN/m and 26.6 mN/m, respectively (Joshi et al., 2013; Amodu et al., 2014).

Nitrogen is the second most important nutrient source after carbon for microbial growth and biosurfactant production. It is also required in large quantities for the biosynthesis of essential cellular substances such as amino acids and purines, including DNA and RNA. Microbial cells' organic compounds contain nitrogen in reduced forms such as amino groups that microorganisms can use as an alternative energy source. Microorganisms mostly use nitrogen in its inorganic state. In most instances, the nitrogen source is reduced to a nitrate prior to utilisation. However, some microorganisms lack the ability to reduce the nitrogen. In such cases, the nitrogen source can be supplied to the microorganisms in a reduced state, using organic nitrogen sources such as urea (Pohlscheidt et al., 2013).

For biosurfactant production, a nitrogen source can be used as a protein component required for the growth of the microorganisms and for enzyme production. Biosurfactant production media can be supplemented by a variety of nitrogen sources such as peptone, ammonium sulphate, ammonium nitrate, sodium nitrate, malt extract, as well as yeast extract, which is the most commonly used (Saharan et al., 2012). Lichenysin production by *Bacillus licheniformis* BAS50 had a two- to four-fold increase upon addition of L-glutamic acid and L-asparagine to the growth media (Yakimov et al., 1998). It has been reported that nitrogen limitation increases biosurfactant production and also changes the composition of the biosurfactant. Val-7 or Leu-7 in a surfactin structure was determined to be influenced by L-amino acid concentration in the medium (Desai & Banat, 1997). It can be deduced that biosurfactant peptide positioning can also be varied by using different nitrogen sources as previously explained in Section 2.2.2, particularly during the stationary phase, when most of the biosurfactant in a culture is produced. Hommel (1990) also proposed that it is the type and not the concentration of the nitrogen source that is important for biosurfactant yields, while the concentration of hydrocarbon sources is responsible for the biosurfactant production**.**

Metallic ion concentrations serve as an important factor in biosurfactant production. They form co-factors for many enzymes responsible for biosurfactant production. Increased biosurfactant production by *Bacillus megaterium* was favoured in a mineral salt medium containing Fe^{2+} ions (Rangarajan et al., 2013). According to Maqsood and Jamal (2011), Fe^{2+} is a co-factor for the enzyme isocitrate lyase involved in cell growth on hydrophobic substrates. Additionally, biosurfactant production by *Pseudomonas aeruginosa* OCD was observed to be enhanced by the addition of Zn^{2+} and Mn^{2+} in the culture medium. Moreover, surfactin production by *Bacillus subtilis* MTCC 2423 increased with the addition of metal supplements such as magnesium (Mg), calcium (Ca), iron (Fe), and other trace elements (Makkar & Cameotra, 2002).

2.4 Biosurfactant applications

2.4.1 Environmental applications

Organic and inorganic compounds released into the environment by industrial activities are difficult to remediate as these easily bind to solid matrices. Biosurfactants increase the bioavailability of these environmental contaminants to the biodegrading microorganisms by mobilisation or increasing pseudo-solubilisation and emulsification. The removal of metal ions through chelation and removal by other chemical reactions between the amphiphiles and metal ions can be achieved by the use of biosurfactants. The amphiphilic part of the biosurfactant alters the physiochemical conditions at the interfaces of solid matrices, modifying the distribution and availability of the environmental contaminants. Additionally,

organic compounds, bacteria, soil particles, water, air, immiscible liquid and the type of hydrocarbon influence the remediation of the hydrocarbon-contaminated soil.

The hydrocarbon can then be solubilised in water, after being adsorbed from soil particles, subsequent to adsorption to cell surfaces followed by biodegradation. When in contact with a contaminant, the biosurfactants can form micelles and emulsify the contaminant. The contaminant partitions in the biosurfactant's micelle core consequently increase contaminant availability, a process that enhances biodegradation. Refer to Table 2.1 for biosurfactant-producing microorganisms employed in environmental bioremediation.

2.4.2 Biosurfactants in nanobiotechnology

The biochemical properties of biosurfactants as well as their self-assembling abilities have been exploited in the field of nanotechnology for development of nanoparticles. Fracchia et al. (2012) reported the synthesis of silver nanoparticles using biosurfactant produced with a low-cost medium by *Pseudomonas aeruginosa*. The nanoparticles were synthesised in biosurfactants' reverse micelles using $NaBH_4$ as a reducing agent (Farias et al., 2014). The micelles act as nano-reactors to facilitate crystal growth, resulting in controlled sized nanoparticles of uniform morphology. The water content within the micro-emulsions can control the morphology and size of the nanoparticles. Higher concentrations of biosurfactants reduce micelle size, thereby decreasing particle size. Nascent nanoparticles are very unstable and prone to aggregation into larger particles. The interactive forces of the micelles cause collision among the micelles, resulting in the exchange of water content with the nanoparticles, which grow to a size controlled by the water core of the micro-emulsion. When the particles reach the size of the water core, the biosurfactants adsorb onto the particle surface. This provides a protective shell around the nanoparticles, preventing aggregation due to electrostatic forces of attraction (Kiran et al., 2011). This shows that the use of biosurfactants for the synthesis of nanoparticles is feasible. It is also interesting to note that nanoparticles can also be used to improve biosurfactant production, owing to their interaction with microbial biomass. For example, iron (Fe^{2+}) nanoparticles increased glycolipid biosurfactant yield by 80% produced by marine *Nacardiopsis* sp. MSA13A (Kiran et al., 2011).

2.5 Nanotechnology in biotechnology: Emergence of nanobiotechnology

The emerging field of nanobiotechnology focuses on the active integration of microbial biotechnology and nanotechnology. Microorganisms' ability to detoxify the environment by reducing heavy toxic metals into metal ions by using reductase enzymes has been exploited for the synthesis of nanoparticles. Biosurfactants can be used as a reducing and stabilising agent in chemical reduction methods of nanoparticles' synthesis. The method of synthesising nanoparticles using biological agents is called green synthesis of nanoparticles. This method

aims to reduce hazardous waste disposed in the environment and costs involved using conventional methods.

Nanoparticles refer to particle size with at least one dimension being between 1 to 100 nm. They are highly reactive compared with their normal particle size; this is because they have a much greater surface area in their nano form. Their nano size has attracted great interest in the field of nanobiotechnology, conferring unique properties that can be exploited. The characteristics of nanoparticles depend on the particle size, shape and composition (Płaza et al., 2014). These desirable properties provide solutions for wastewater treatment, medicine, and pharmacological challenges. They also aid in the bioprocessing of agrowaste to useful by-products. They have been widely exploited as enzyme immobilisers in SSF owing to their large surface area and recoverability (Kalska-Szostko et al., 2012).

2.5.1 Synthesis of nanoparticles

Nanoparticles are synthesised by many different physical and chemical methods. They can either be synthesised using a top-down approach which involves the breaking down of the normal particle size into nano size, or a bottom-up approach, whereby atoms are assembled to molecular structures that fall within the nano range (Płaza et al., 2014). Physical methods include plasma arching, ball milling, thermal evaporation, spray pyrolysis, pulsed laser desorption, lithographic techniques, sputter deposition, layer by layer growth, molecular beam epistaxis and flame diffusion. Chemical methods include electro-deposition, sol-gel processing, chemical solution deposition, chemical vapour deposition, soft chemical usage, Langmuir–Blodgett method, catalytic route, hydrolysis, and the co-precipitator and wet chemical methods.

The most commonly used method is the chemical reduction method that involves reducing metal salts to metal atoms by using a reducing agent. The synthesis of nanoparticles has been a serious challenge for many years in the attempt to promote green chemistry. The currently employed chemical and physical processes are labour intensive and use high radiation, temperature and pressure, as well as highly concentrated toxic chemicals as reducing and stabilising agents; these can become a threat to the environment and living organisms when disposed off in the environment. Research has focused on the development of clean, non-toxic and environmentally safe production processes for synthesis of nanoparticles. There have been many reported attempts at synthesising nanoparticles in supposed environmentally friendly, non-toxic processes that promote the green chemistry approach.

In a study by Gan et al. (2012), palm oil mill effluent was used as a reducing agent for the synthesis of gold nanoparticles from a chloroauric acid solution ($HAuCl_4$) as a source of the

metal precursor. However, this approach still produces toxic chemical waste from the source of the metal precursor. Similarly, Le et al. (2013) produced silica nanoparticles from Vietnamese rice husks as a source of metal precursor but used analytical grade chemicals as reducing and stabilising agents. These studies represent limitations when green chemistry is used. Therefore, there is a need to refine this approach by using renewable resources such as agrowaste for the whole process being developed.

2.5.1.1 Characterisation of nanoparticles

Characteristics of nanoparticles can be determined by using various microscopic and spectroscopic techniques. Characterisation allows control over synthesis and applications of nanoparticles. For microscopic analysis of nanoparticles (owing to their small particle size), microscopes with higher resolution using an electron beam are employed. Electron microscopes such as the Transmission Electron Microscope (TEM) and Scanning Electron Microscope (SEM) are the most commonly used. These microscopes are ideal for nanoparticle characterisation owing to their use of electron beams and electromagnetic radiation with a shorter wavelength. Nanoparticles cannot be observed with light microscopes because of their diffraction effect. The electron beam interacts with the sample and can either be transmitted, backscattered or diffracted with all these signals being measurable. The SEM measures electrons that are backscattered and electrons emitted from the sample and the TEM measures the transmitted electrons by the sample. The difference between the TEM and SEM is the signal measured. The TEM is more suitable for particle size analysis because of its high resolution, whereas the SEM is suitable for surface and shape analysis.

2.5.1.1 (a) Transmission Electron Microscope (TEM)

The TEM is made up of three essential systems: a condenser system, image-producing system and image-recording system. All systems are responsible for the direct imaging of the nanoparticles. Electrons are produced in a V-shaped tungsten cathode filament known as the electron gun. In between the electron gun and the specimen is a condenser system that intensifies the electrons to focus the beam on the object. A highly magnified image is produced in the image-producing system that is made up of an objective lens, movable specimen stage, and intermediate and projector lenses that focus the electrons interacting with the specimen.

2.5.1.1 (b) SEM, UV-Vis and X-ray diffraction

Electrons in SEM are of high energy and generate signals on the surface of a solid specimen. The apparatus and systems of the SEM are relatively similar to those of the TEM with the electron gun being the source of electrons. The energy carried by the electrons is

dissipated upon interaction with the sample, generating various signals. SEM images are obtained from these signals, more especially secondary and backscattered electrons. Secondary electrons show morphology and topography on samples and backscattered electrons reveal contrast in composition in multiple-phased samples. Other signals generated in the SEM include diffracted backscattered electrons, visible light, heat and photons.
As for photons, they generate X-rays with a fixed wavelength when the electrons reach a lower energy state. These X-rays can be used for elemental analysis as different X-rays are produced for each element in a mineral (University of Essex, 2014).

The major setback in using the TEM and SEM for nanoparticle characterisation is that it is uncertain that the generated images are representative of the bulk sample of the nanoparticles (Herrera & Sakulchaicharoen, 2009). Therefore, complementary and more sensitive methods that provide structural properties and quality are employed. In this case, X-ray diffraction (XRD) is used because of its ability to analyse polycrystalline materials to determine the crystallinity of particles. The incident X-rays are scattered by the sample's atoms and interfere with one another. This interference is analysed by using Bragg's law to determine the polycrystalline material's characteristics. Nanoparticles can also be characterised using spectroscopic techniques such as the Fourier Transmission Infrared (FT-IR) to determine functional groups involved in the bioreduction of metals and ultraviolet visible light (UV-Vis) to determine distribution of the nanoparticles. Spectroscopic techniques are based on a light absorption technique. They provide information on dispersion of nanoparticles, local structures formed by transition metals oxides, sulphides and selenides (Herrera & Sakulchaicharoen, 2009).

2.5.1.2 Purification and separation of nanoparticles

There are many different methods currently employed for size- and shape-selective purification of produced nanoparticles. Purification methods include chromatography, electrophoresis, centrifugation and filtration. Separation of nanoparticles is a very critical step post synthesis. Polydiversity affects the size-dependent properties of individual nanoparticles. Hanauer et al. (2007) successfully separated gold and silver nanoparticles based on their size and shape by gel electrophoresis. This was achieved by coating the nanoparticles with a charged polymer. In electrophoresis, the charged coated particles are subjected to a uniform electric field. The charged particles migrate towards the opposite polarity electrode. Particles migrate at different velocities according to their size and shape. Furthermore, size exclusion chromatography is the most applicable chromatographic technique for separation of nanoparticles. Separation using size exclusion chromatography is based on particles' hydrodynamic volumes. In contrast, chromatographic techniques such as high-performance liquid chromatography (HPLC) separation are based on partition

coefficients between the mobile phase containing the nanoparticles mixture and the stationary phase (Kowalczyk et al., 2011). The other form of separation technique used for purification of nanoparticles is density gradient centrifugation.

This technique depends on the density of the particles, with particles denser than a liquid matrix settling. The forces applied by centrifugation allow particles to separate according to size and shape. Other separation techniques include selective precipitation, which separates nanoparticles according to reactivity, stability, including size-dependent physical and chemical properties. Additionally, membrane size filtration, which depends on membrane pore size, can be used. There are also other extraction methods based on particles' suspension in water and organic solvents (Kowalczyk et al., 2011).

2.5.2 Green synthesis and bio-reduction mechanisms for nanoparticle production

Current trends focusing on the green synthesis of nanoparticles include using plant extracts for the synthesis of metal nanoparticles. This is due to their biodiversity and availability (Kuppusamy et al., 2014). Plant extracts are also known to have secondary metabolites with desirable properties for nanoparticle synthesis. Plant metabolites such as sugars, terpenoids, polyphenols, alkaloids, phenolic acids and proteins (Makarov et al., 2014) contain functional groups such as C=C (alkenyl), C=N (amide), O=H (phenol and alcohol), H-H (amine) C-H and COO^- (carboxylic acid groups) (Kuppusamy et al., 2014), which can be exploited for both biosurfactant and nanoparticle synthesis.

The ability of plants to bioaccumulate and deposit metals in a form of nanoparticles has led to the discovery of the usefulness of their reductive metabolites. Nanoparticles recovered from plants by sintering and smelting methods are not industrially applicable. The morphology and size of these nanoparticles vary depending on the plant organ they are deposited from. For industrial purposes, application of the nanoparticles requires finely tuned sizes and shapes. Currently employed in-vitro synthesis of nanoparticles has shown better results (Makarov et al., 2014). It involves metal salts and a plant extract for bioreduction of the desired metal to nano size. This approach allows for the control of size and morphology of the nanoparticles being produced. Desirable size and shape of nanoparticles can be obtained by altering the pH of the medium, reaction time, temperature, metal concentration and the quantity of the plant extract used (Kuppusamy et al., 2014; Makarov et al., 2014).

During nanoparticle synthesis, metal ions undergo different phases. The first phase is called the activation phase where the metal ions are reduced to their metal atoms followed by nucleation of the atoms. Upon nucleation, isolated nanoparticles amalgamate into a larger particle size following a process called Ostwald ripening. This is a process whereby

synthesised nanoparticles undergo nucleation and aggregation into specific shapes. This phase is called the growth phase, a phase that increases the thermodynamic stability of the nanoparticles produced.

Thereafter, the termination phase is initiated after the growth phase, whereby the nanoparticles are subjected to conformation by profusely high favourable energies. This phase is mediated by the plant extract's ability to stabilise the nanoparticles (Makarov et al., 2014).

FTIR analysis of metal nanoparticles synthesised in a green synthesis method has been found to be associated with plant extracts during such a synthesis (Makarov et al., 2014). As previously discussed, plant metabolites such as terpenoids, reducing sugars, alkaloids and phenolic acids can play an important role in the synthesis of nanoparticles. Terpenoids are natural compounds with five carbon isoprene units, with strong oxidising and antioxidant activity. For the reduction of the metal, a proton dissociates from the active functional group, resulting in an oxidising resonance structure accompanied by reduction of metal ions to nanoparticles. Interestingly, polyphenolics, a large group of compounds comprising several classes, namely, anthocyanins, isoflavonoids, flavanols, chalcones, flavones, and flavonoids, have different reducing mechanisms compared with terpenoids. Flavonoids reduce metals by chelation with their carbonyl groups or Ω electrons. Some FTIR results showed that flavonoids adsorbed onto the nanoparticles' surface. Moreover, flavonoids undergo tautomeric transformation from an enol to a keto form, realising a reactive hydrogen species which in turn reduces the metal ions into nanoparticles (Makarov et al., 2014).

2.5.3 Factors affecting nanoparticle synthesis using plant extracts

There are many factors that affect the bioreduction of metal ions to nanoparticles. Factors such as the pH of the medium determine the plant extract's ability to bind and reduce metal ions. Furthermore, a change in pH affects the charge and properties of the phytochemical extract. At alkaline pH, plant extract functional groups become negatively charged and efficiently bind and reduce metal ions. Alkaline conditions have an effect on the morphology, size and yield of nanoparticles (Makarov et al., 2014). Vanaja et al. (2013) demonstrated the effect of pH on the synthesis of silver nanoparticles using a *Coleus aromaticus* leaf extract, whereby an alkaline pH favoured silver nanoparticle synthesis. At low pH, small broadening of the surface plasmon resonance peak was observed, an indication of large-sized particle synthesis. According to Makarov et al. (2014), under acidic conditions, minimal nucleation occurs which favours agglomeration of metals giving large particles, a limitation associated with the use of plant extract under such conditions.

Temperature has also been reported to have an adverse impact on the synthesis of nanoparticles (Lee et al., 2014). Higher temperatures increase the efficiency of nanoparticle synthesis and the rate of reaction. Furthermore, crystalline particles are formed more efficiently at high temperatures than at room temperatures. Elevated temperatures increase the rate of nucleation of the metal atoms into nanoparticles. However, extremely high temperatures have an adverse effect on the morphology of the nanoparticles. Higher temperatures affect the interactions of the plant's phytochemical and the nanoparticles' surface chemistry, inhibiting the growth phase during nanoparticle formation (Makarov et al., 2014). Nanoparticle synthesis is also affected by the electrochemical potential of an ion. Effective metal ion reduction is favoured for metal ions with a large positive electrochemical potential rather than for a metal ion with a low electrochemical potential (Makarov et al., 2014).

2.6 Agrowaste as a feedstock for bioprocesses

Agrowaste is the by-product of industrial processing of agricultural produce. The agrowaste generated is known to be the most abundant renewable resource. The waste is of great economic and environmental interest because of its availability in large quantities and its composition. Agrowaste can be used as a low-cost material for the production of other useful compounds, thereby reducing production cost. The use of agrowaste material limits the disposal of waste containing phenolics and other toxic compounds into the environment (Bhatia et al., 2012).

Agrowaste biomass is comprised of lignocellulosic material which is abundant in various sources in the environment and a portion of it is used in the production of fertilisers; however a large portion is volatised or left to decay (Saini et al, 2014). This type of waste is inexpensive and applicable on a large scale. It is also cost effective for bioproduct production, particularly for processes classified as low-performance fermentations.

2.6.1 Lignocellulose biomass

Lignocellulosic biomass consists of three compounds that make up its structure, namely, cellulose, hemicelluloses and lignin. It also contains small quantities of proteins, although these are not involved in structure formation. Cellulose is the core part of the structure that retains the crystalline fibrous structure with hemicelluloses within the micro and macrofibrils of cellulose; both are embedded in lignin, which provides the structural integrity of the entire matrix (Anand et al., 2013). Agricultural lignocellulosic biomass contains 10 to 25% lignin, 20 to 30% hemicelluloses and 40 to 50% cellulose. However, lignocellulosic composition depends on the source, which can either be hard wood, soft wood or grass, even in agrowaste.

2.6.1.1 Lignin in agrowaste

Lignin is a complex of tree phenyl-propane units, *p*-coumaryl, coniferyl and sinapyl alcohols linked by ether bonds (Anand et al., 2013; Anwar et al., 2014). It is also made up of methoxy groups and non-carbohydrate polyphenol substances that bind the cell walls (Anwar et al., 2014). Lignin is synthesised in a process called lignification.

During lignification, monomeric phenyl is polymerised in the cell wall, producing radicals that are coupled with other monomeric radicals through oxidative coupling, resulting in bond formation. The outcomes in the formation of a long chain heterogeneous polymer of phenyl-propane groups produce a lignin compound structure. It is the most abundant hydrophobic and aromatic polymer in agrowaste. Microorganisms that secrete lignase enzymes can degrade lignin, including peroxidises and cellobiose dehydrogenase. These oxidative enzymes are involved in the biodegradation of the complex structure of lignin, the residual cellulose being left intact (Mussatto & Teixeira, 2010). The characteristics of these enzymes differ greatly, depending on microbial origin. Lignin peroxidases are one of the most important types of ligninases involved in the biodegradation of lignin. They have the ability to cleave the non-phenolic units that make up 90% of the lignin structure, including the propyl side chain of lignin. Manganese peroxidases are the second most important enzymes found to facilitate lignin degradation, as they degrade non-phenolics in the lignin matrix (Mussatto & Teixeira, 2010).

2.6.1.2 Cellulose and hemicelluloses in agrowaste

In agrowaste, cellulose and hemicelluloses are the main sources of fermentable sugars (Mussatto & Teixeira, 2010). Hemicelluloses are made up of repeated pentose and hexose polymers. On the other hand, cellulose is a very stable polymer of repeating glucose monomers. The glucose monomers are held together by inter- and intramolecular hydrogen bonds, resulting in the rigidity of the structure. Hemicelluloses and cellulose are bound together by non-covalent interactions embedded within the lignin matrix (Anwar et al., 2014). This makes cellulose less accessible. Also, its compact, rigid structure and complex interlocked structure with hemicelluloses, lessens reactive sites for enzyme attachment and action. Enzymes involved in cellulose biodegradation are cellulolytic enzymes. Cellulolytic enzymes are multi-enzyme complexes consisting of three major types, cellobiohydrolase, endo β-glucanase and β-glucosidase. They synergically hydrolyse cellulose and produce glucose, cellobiose and other oligosaccharides (Mussatto & Teixeira, 2010), which are fermentable. Microorganisms can produce suitable enzymes for both delignification and biosurfactant production, but confirmatory biochemical tests must be conducted to ascertain the ability of the biocatalyst to perform both tasks.

As such, biosurfactant production using unconventional substrates is viable and is considered an economically feasible method. Agrowaste is a perfect substitute for conventional substrates as it also contains the requisite carbohydrate and lipid balance, including trace elements required for microbial growth, which can enhance biosurfactant production (Nitschke et al., 2004).

Successful studies have been carried out to develop economical methods for biosurfactant production by the use of unconventional substrates. A study carried out by Płaza et al. (2011) showed that *Bacillus* strains were able to produce biosurfactant using agrowaste as a substrate. Some *Bacillus* strains grew well on two brewery effluents and on molasses, as well as on fruit and vegetable waste. Molasses, fruit and vegetable agrowaste was found to contain high nutritional components for biomass growth. Many unconventional substrates have been assessed for microbial growth and subsequent biosurfactant production (see Table 2.1). However, they have been supplemented with commercial growth media to ensure optimal growth and high production yield. Lichenysin biosurfactant with great surface tension reduction activity was successfully synthesised by *Bacillus licheniformis* STK01 using solely *B. vulgaris* agrowaste. Therefore, *B. vulgaris* agrowaste was determined as a suitable agrowaste for biosurfactant production (Amodu et al., 2014).

2.6.2 *Beta vulgaris* agrowaste

2.6.2.1 Nutrient components in *Beta vulgaris*

B. vulgaris is a type of agrowaste material that is a rich source of valuable compounds. It is an herbaceous biennial from the Chenopodiaceae family (Singh & Hathan, 2014). Nutritional analysis of *B. vulgaris* by Shyamala and Jamuna (2010) revealed that it has a moisture content of 79% and ash content of 6.18%, with a high mineralogical content as a source of micronutrients. It also serves as a rich source of calcium and phosphorus. Elemental analysis using ICP-MS by Amodu et al. (2014) reported elements present in *B. Vulgaris* extract as being Ca, Fe, Mg, K, Na, Zn and P. According to Singh and Hathan (2014), *B. vulgaris* is also a rich source of anti-oxidants such as saponins, betacyanines, folates, betanin, polyphenols and flavonoids. It was therefore hypothesised that this type of agrowaste, can be used as a facilitator and primary feedstock for nanoparticle production (Parameshwaran et al., 2013) and biosurfactant synthesis (Amodu et al., 2014).

2.6.2.2 Betanin in *Beta vulgaris*

Betanin is the red dye that gives *B. vulgaris* its purple-red colour. It belongs to a group of natural pigments called betalains. Betalains contain nitrogen-based pigments which are water soluble. They can be sub-divided into two classes, betacyanins and betaxanthins (Neagu & Barbu, 2014). This group of nitrogen-containing pigments is synthesised from the

amino acid tyrosine, with betalamic acid being the chromophore found in all betalain pigments. The betalamic acid content determines the classification of the pigment (De Azeredo et al., 2009). The difference between the two classes is the conjugation of an aromatic nucleus to the chromophore present in betacyanine, giving a red purple pigmentation absent in betaxanthins which give a yellow pigmentation (Attia et al., 2013). *B. vulgaris* is reported to be the main source of both classes of betalains (De Azeredo et al., 2009).

Betanin, a betacyanine, is the principal pigment accounting for 75% to 95% of *B. vulgaris* pigment (Wybraniec & Michałowski, 2011). Betalains can also be found in roots, fruits and flowers (De Azeredo et al., 2009) situated in cell vacuoles (Neagu & Barbu, 2014). In *B. vulgaris,* betacyanine can be obtained from press juice or aqueous extraction of shredded agrowaste (Singh & Hathan, 2014). Various studies have reported on the stability of betalain (De Azeredo et al., 2009; Attia et al., 2013). However, the stability of betalains is affected by pH, temperature, oxygen, light and metals. Attia et al. (2013) reported that betalains subjected to various pH, almost 93% to 100%, remained stable at acidic and neutral pH. De Azeredo et al. (2009) further elucidated that at alkaline pH, the amine bond in betalains is hydrolysed, whereas in acidic pH, recondensation of betalamic acid occurs.

The colour of betalain changes when heated; the rate of betalain degradation increases at higher temperatures; therefore, the maximum stability of the pigment has been reported to be 40 to 50 ˚C with accelerated degradation rates occurring at temperatures above 70 ˚C (Attia et al., 2013). De Azeredo et al. (2009) further proposed that at high temperatures, betanin is degraded via isomerisation and decarboxylation, conditions also influenced by pH. However, C_{15} isomerisation or decarboxylation does not result in significant colour change and light absorption characteristics. In contrast, C_{17} decarboxylation caused hyposochromic shift of light absorption, giving an orange-red appearance. Dehydrogenation of betanin results in neobetanin formation, giving off a yellow colour. Bond cleavage of betanin releases betalamic acid, resulting in a bright yellow colour and a colourless cyclo-Dopa-5-O-glycoside (De Azeredo et al., 2009). The chemical structure of Betanin is shown in Figure 2-3.

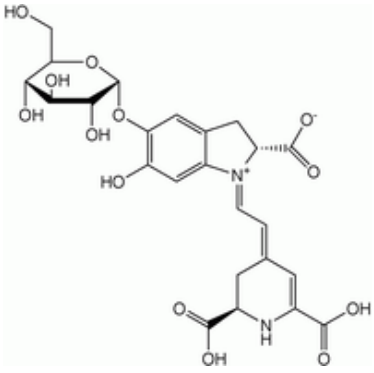

Figure 2-3: Chemical structure of betanine

2.7 *Bacillus* spp.*:* A suitable biocatalyst for biosurfactant production

2.7.1 *Bacillus* genus and taxonomy

The genus *Bacillus* is a very large and diverse group of gram-positive, rod-shaped, spore-forming, catalase-producing species (Maughan & Van der Auwera, 2011). Initially, there were 145 species in this genus, with differences focusing on phenotypic characteristics, DNA base composition and DNA–DNA hybridisation with 40 species being identified. They are distinguished from other Bacillaceae members by their nature; either aerobes or facultative anaerobes. This has been a genus of interest for many years, owing to its ability to produce a multitude of bioproducts with a chemically resistant refractive endospore structure and pathogenicity of the species.

This genus consists of different microorganisms possessing different ecological and physiological characteristics, each occupying different habitats depending on environmental conditions. They have been isolated in different areas that include fresh water, saline water, soil, plant roots/parts, and on animals and in air as bioaerosols. They are very ubiquitous in nature, encompassing spectacular phenotypic traits, tolerance of high temperatures, extremes of salinity and acidic conditions. Contributing to the diversity of the genus is the unusual ability to act as an electron acceptor (Maughan & Van der Auwera, 2011). A range of physiological characteristics includes the ability to utilise a variety of substrates, production of high-volume products such as antibiotics, heterotrophic nitrifiers, denitrifiers, nitrogen fixers, and iron precipitators, and they can act as oxidisers and reducers. The genus has representatives in facultative chemolithotroph, acidophile, alkanophile, psychrophile and thermophile classes (Slepecky & Hemphill, 2006). For the purpose of this study *Bacillus* sp. has also been identified as a biosurfactant producer.

2.7.2 Isolation and identification of individual *Bacillus* species

Different techniques have been employed to study the *Bacillus* taxonomy, isolation methods and the determination of individual species. Guanine and cytosine (GC) content analysis and DNA hybridisation experiments revealed the heterogeneity of the genus. The *Bacillus* species was determined to have a low GC content (Maughan & Van der Auwera, 2011), ranging from 32% to 69% (De Boer et al., 1994). Analysis of strains at a genetic level revealed the varying extent of their biochemical, morphological, physiological and chemo-taxonomical traits (Fritze, 2004).

There are two successfully used taxonomic methodologies. The first is the isolation and enrichment process to determine physiological, nutritional and cultural requirements of the microorganisms; however, this technique is not very accurate. The second methodology is based on the analysis of the 16S rRNA/DNA sequence. Analysis of the 16S rRNA sequence is the most effective approach to identify the large *Bacillus* taxonomy. The 16S rRNA is mostly used for taxonomic purposes as it is the most conserved sequence and serves as a critical component of the cell function. Common gene enzymes among species could be ideal for taxonomic identification; however they are subject to mutations, although the rate of changes in the 16S rRNA gene sequence is not known (Iii, 2004).

Analysis of the 16S rRNA is advantageous as it allows the identification of new genera within already existing genera; this facilitates the discovery of novel genera to identify new species. Price et al. (2009) aligned 7510 16S rRNA sequences for comparisons and investigated possible relationships with the closely related *Listeria* genera. By using TreeChopper® software, they identified 97% of the 7510 analysed 16S rRNA sequences, resulting in the conclusion that only 116 *Bacillus* species exist. This technique includes isolation of genomic DNA of investigated microorganisms, and amplifying the 16S rRNA gene by Polymerase Chain Reaction (PCR). PCR is a mass amplification technique of a target sequence determined by primers, a short segment of nucleotides complementary to the section of the DNA to be amplified. It is a rapid and easy method for generating unlimited copies of any fragment of isolated DNA (Iii, 2004).

2.7.3 *Bacillus licheniformis:* A biosurfactant-producing species

Bacillus licheniformis is a gram-positive spore forming saprophytic bacterium. It belongs to group VI of the *Bacillus* genus along with *Bacillus subtilis* and *Bacillus amyloliquefaciens.* It is physiologically similar to other species in the genus such as *Bacillus pumilus and Bacillus astrophaeus.* These are phenotypically closely related species but genotypically distinct. *Bacillus licheniformis*, in particular, has only 10% DNA homology with other species in the *Bacillus* genus and was found to be closely related with *Bacillus amyloquefaciens* with 9% to 15% homology to *Bacillus pumilus* (De Boer et al., 1994).

Commonly found in the natural environment, it dominates nutrient-poor soils such as moorlands and deserts (De Boer et al., 1994), with optimal growth temperature of 30 ˚C. It is also known to survive extreme temperatures (Dewaliya & Jasodani, 2012). It attracts great interest as a biocatalyst for industrial purposes, because of its ability to produce biotechnologically useful products. Also, it is found to test positive for various biochemical tests, can grow anaerobically, facilitate arginine dehydrolase production and starch hydrolysis (De Boer et al., 1994).

Hence, it has the ability to degrade several substrates and grow in a variety of nutrient sources, including agrowaste. This is largely made possible by its ability to produce and secrete hydrolytic enzymes.

This bacterium is non-pathogenic to humans and is considered safe for industrial use. Its attractiveness is owed to its simple growth requirements and secretion of proficient quantities of protein, including bioinsecticidals (Płaza et al., 2014). There have been reports on its ability to produce industrially important commercial enzymes, for example, alpha amylase, that has been tested on different agricultural by-products and found to be suitable for optimal production of amylase (Divakaran et al., 2011). Keratinase was also isolated from a culture medium of feather-degrading *Bacillus licheniformis.* Again, *Bacillus licheniformis* has shown its ability to facilitate the production of nanoparticles through the production of a biosurfactant (Płaza et al., 2014).

Another very important attributes of *Bacillus licheniformis* is its ability to produce cyclic lipopeptide biosurfactants utilising either carbohydrates or hydrocarbons. Cyclic lipopeptide were reported to be first produced by members of *Bacillus* sp. producing surfactin-like biosurfactants which still are one of the most effective biosurfactants reported to date (Thaniyavarn et al., 2003; Gudiña et al., 2015). *Bacillus licheniformis* has been reported to produce the lipopeptide lichenysin biosurfactant with a lipid moiety of fatty acids and amino acids which has proved to be a very efficient surfactant with antimicrobial activity (Burgos-Díaz et al., 2012).

Additionally, different strains of *Bacillus licheniformis* have been identified to produce biosurfactants. *Bacillus licheniformis* F2.2 was identified as a biosurfactant-producing strain that was isolated in fermented food in Thailand. This strain was found to produce a new biosurfactant code, named BL 1193, as well as two lipopeptide biosurfactants, plipastatin and surfactin, which were produced abundantly in a YPD medium, while BL 1193 was produced in an amino acid-free synthetic medium (Thaniyavarn et al., 2003).

Microorganisms producing biosurfactants are required to change surface and interfacial properties of the surrounding environment. For efficient cell growth, microorganisms interact with essential nutrients within such surroundings, a process facilitated by the produced biosurfactants. They are therefore produced when they encounter an unmodified interface, regulating metabolic interaction of the microorganisms with surfaces, particularly solid substrates, such as agrowaste. Surface interfacial interactions are needed in the complex microbial responses that control cellular development.

Most importantly, microorganisms produce biosurfactants to improve mass transfer processes such as gliding and swarming, including re/de-attachment to and from solid matrices, and cell–cell interactions to improve biofilm formation and maintenance. In biofilms, biosurfactants also contribute to the nutritional balance of the biofilm at different depths and prevent invading bacteria from colonising the available spaces in the resident biofilm (Burgos-Díaz et al., 2012).

2.7.3.1 The genome of *Bacillus licheniformis*

The complete genome of the different strains of *Bacillus licheniformis* has been well studied in comparison with the well-studied *Bacillus subtilis* (Rey et al., 2004). There are established co-linear regions between *Bacillus licheniformis* and *Bacillus subtilis*. The two industrially important bacteria were found to be 70% identical at the nucleotide levels. Complete genome sequencing of two different *Bacillus licheniformis* strains, DSM13 and ATCC 14580, was conducted by Veith et al. (2004) and Rey et al. (2004). Both findings suggested that the *Bacillus licheniformis* genome consists of one circular chromosome made up of 4222000 bp with slight variations among different strains.

The two strains had a common GC sequence, which determines the average GC content of the bacterium at 46.2%. This finding agrees with those reported by Yangtse et al. (2012) for *Bacillus licheniformis* WX-02.

All of the reported strains, ATCC 14580, DMS13 and WX-02 genome analysis revealed that *Bacillus licheniformis* consists of 7 rRNA operons and 72 tRNA genes. The number of open reading frames (ORF) varies among strains. The ATCC 14580 strain was predicted to be 4208bp. This was determined by both manual inspection and gene-finding programs. ORFs in WX-02 were identified using FgenesB, Prodigal and Glimmer gene-finding programs with 4320 ORFs being identified. It was suggested that the DSM13 strain has 74.3% ORFs which are located on the leading strand. Rey et al. (2004) further extrapolated from their findings that the identified ORFs are 873bp on average. They are allocated in the direction of replication on the chromosome. This concurred with the findings and/or assertions of Veith et al. (2004) that 74.4% of genes are located on the leading strand with 25.6% on the lagging strand.

2.7.3.2 *Bacillus licheniformis* STK 01

A novel biosurfactant-producing strain was discovered in a study conducted by Amodu et al. (2014). The strain was isolated from rotting wood and grown exclusively on agrowaste, that is, *B. vulgaris,* as a sole carbon source to produce biosurfactants. The strain was morphologically identified as a spore-forming gram-positive *Bacillus* sp. with reddish-pink rod-shaped colonies. It was also identified by 16S rRNA sequence analysis.

It was identified as *Bacillus licheniformis* designated as strain STK 01 and found to be closely related to three other strains of *Bacillus licheniformis*: strains ZML 1, SCCB 37 and 1 FTM8. The biosurfactant produced demonstrated a high propensity for hydrocarbon emulsification and surface tension reduction of water to below 30 mN/m.

This was claimed to be one of the highest surface tension reductions for a biosurfactant produced using agrowaste solely without any supplements with refined substrates. *B. vulgaris* agrowaste was reported for the first time as a sole substrate, suggesting the novelty of this strain. The strain produced emulsification activity results comparable to studies reported for biosurfactant produced using refined substrates. The biosurfactant was found to be a lichenysin cyclic LMW lipopeptide, based on an FTIR analysis report.

2.8 Summary

Industrial activities such as mining, petrochemical and petroleum processing produce a large quantity of hazardous waste that is most likely to end up in the environment. Remediation of contaminated sites is a necessity, as such waste may impacts negatively on environmental health. Petroleum- based chemical surfactants have been extensively used for remediation of contaminated sites. Upon remediation, the surfactant residue remains in the environment, posing the risk of considerable damage to the environment.

The research focus of environmentalists has been on the development of environmentally friendly alternative surfactants. Microbial-based surfactants, that is, biosurfactants, are potential alternatives to the currently used petroleum- based chemical surfactants. The limitations on the use of biosurfactants are high production costs and low production yield. To reduce production costs, agricultural waste can be used as substrate for biosurfactant-producing microorganisms. Agrowaste material is rich in lignocellulosic material, cellulose and hemicelluloses being the main sources of fermentable sugars. To improve production yield, the field of nanobiotechnology provides possible innovative solutions for improving bioprocess conditions by direct application of nanomaterials. Nanoparticles have been successfully employed to enhance biosurfactant production. The major drawbacks to the application of nanoparticles are the methods used. The synthesis of nanoparticles uses high pressure and temperatures, and synthetic petroleum-based chemicals that also have an adverse effect on the environment. Recent research has focused on the development of clean, non-toxic, environmentally friendly methods. Plant secondary metabolites have also been used as a replacement for toxic-reducing agents. However, this method still requires the use of strong metal precursors. Alternatively, agrowaste material is known to contain various metals and thus, can be used solely as a source of metal precursors and reducing agents using plant secondary metabolites present in such waste. Figure 2-4 illustrates the process used for this study.

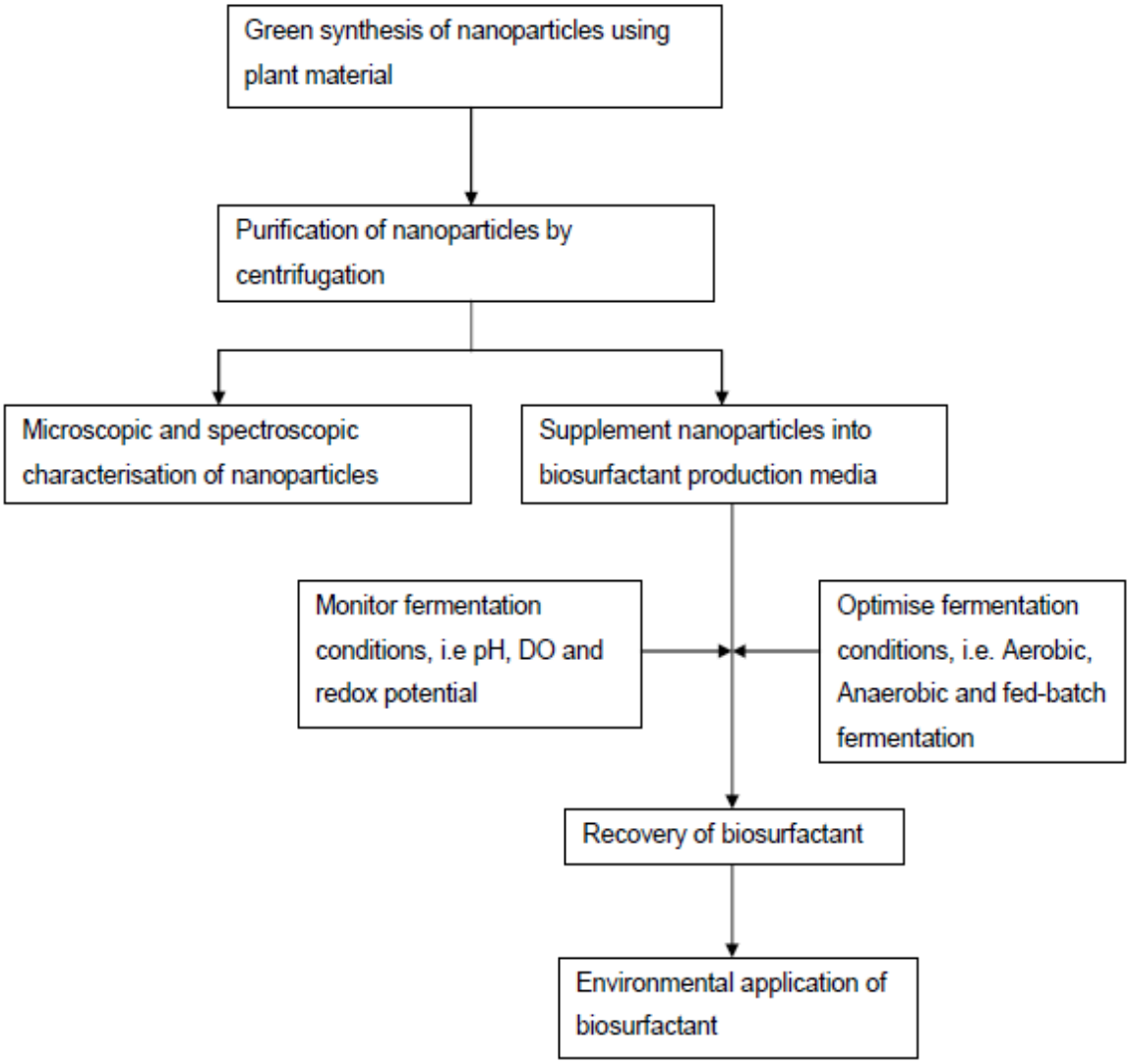

Figure 2-4: Flowchart to implement nanobiotechnology strategies to enhance biosurfactant production

CHAPTER 3
METHODS AND MATERIALS

3.1 Synthesis of nanoparticles

3.1.1 Preparation of *Beta vulgaris* solutions for nanoparticle synthesis

Beta vulgaris (*B. vulgaris*) extract solution was prepared from *B. vulgaris* agrowaste obtained from a fruit- and vegetable-processing facility located in Cape Town, Western Cape, South Africa. The facility is located within close proximity of the Cape Peninsula University of Technology District Six campus. The waste was milled and oven dried at 70 °C for 72 h, and thereafter it was pulverised to a size less than 0.30 mm. A mass of 10 g of the pulverised *B. vulgaris* was added into 1 L of sterile distilled water (sdH_2O). Additionally, a *B. vulgaris* juice extract was obtained by juicing the freshly peeled *B. vulgaris* tubers in a blender (Russell Hobbs™, England), and the removal of agrowaste debris was achieved by filtering the solution through a 125 mm Whatman® filter paper.

3.1.2 Preparation of *Aloe vera* solution to enhance nanoparticle synthesis process

Aloe vera (A. vera) plant extract was obtained within the premises of the Cape Peninsula University of Technology, District Six Cape Town campus. *A. vera* contains bioactive phytochemicals that can facilitate nanoparticle formation. The *A. vera* leaf was cut into small fractions and 20 g of the sliced *A. vera* were added into 200 mL of sdH_2O. An *A. vera* extract solution was prepared by boiling at 100 ˚C for 60 min. The solution was filtered through 125 mm Whatman® filter paper to remove debris prior to usage.

3.1.3 Preparation of $CaCO_3$ solution from eggshells for pH adjustment

Eggshells were obtained from a restaurant on the campus of the Cape Peninsula University of Technology, District Six Cape Town campus. The eggshells were washed in running tap water and oven dried at 70 °C for 24 h and milled to produce a fine powder. A mass of 50 g of powdered eggs shells was added to 100 mL of sdH_2O and autoclaved at 121 °C for 15 min and then filtered through a 125 mm Whatman® paper. The eggshell solution was used to adjust pH.

3.1.4. Optimisation of pH and temperature

Eight samples (1–8) (Table 3.1) were used to optimise pH and temperature for the synthesis of nanoparticles. The pH was tested at acidic (low and high acidity) and alkaline (low/high alkalinity) conditions. The pH adjustment was accomplished by either using 1 M NaOH and/or $CaCO_3$ extracted from the eggshells (for the alkaline study), while 1M HCl was utilised for the studies conducted under acidic conditions. Temperature was tested at room temperature 25˚C (RT) and at 80 °C (Parameshwaran et al., 2013).

The presence and synthesis of nanoparticles were determined by a colorimetric technique from *B. vulgaris* cultures (Kalimuthu et al., 2008) as the interaction of plant extract with metal ions in solution alters the properties of the extract, resulting in a colour change.

3.1.5 The effect of *Aloe vera* on metallic nanoparticle synthesis

The effect of *A. vera* in the synthesis of nanoparticles was evaluated (Sample 9, Table 3.1), with the *A. vera* solution being added to the *B. vulgaris* extract solution at a ratio of 1:1 (see Table 3.1). The $CaCO_3$ solution from eggshell extract solution was used to adjust the pH of the media.

3.1.6 Nanoparticle synthesis from *B. vulgaris* extract solution and juice extract

A comparative study between the *B. vulgaris* extract solution and the *B. vulgaris* juice extract solution was evaluated. Different concentrations of juice extract were evaluated (see Table 3.1). The reaction was carried out at optimised pH and temperature, and the presence was assessed based on the colour change and reaction time.

Table 3.1: Process parameters for the synthesis of nanoparticles

Sample ID	Temperature °C	pH	*B. vulgaris* solution	BV:AV ratio	pH adjusting solution
1	RT	2	10 mL extract solution	1:0	1M HCl
2	RT	6	10 mL extract solution	1:0	1M HCl
3	RT	8	10 mL extract solution	1:0	1M NaOH
4	RT	10	10 mL extract solution	1:0	1M NaOH
5	80 ˚C	2	10 mL extract solution	1:0	1M HCl
6	80 ˚C	6	10 mL extract solution	1:0	1M HCl
7	80 ˚C	8	10 mL extract solution	1:0	1M NaOH
8	80 ˚C	10	10 mL extract solution	1:0	1M NaOH
9	80 ˚C	8	10 mL extract solution	1:1	$CaCO_3$
10	80 ˚C	8	Juice extract	1:0	1M NaOH
11	80 ˚C	8	10 % (v/v) juice extract	1:0	1M NaOH
12	80 ˚C	8	1 % (v/v) juice extract	1:0	1M NaOH
13	80 ˚C	8	0.1% (v/v) juice extract	1:0	1M NaOH

RT: Room Temperature **BV**: *B. vulgaris* **AV**: *A. vera*

3.1.7 Purification and characterisation of nanoparticles

The nanoparticle purification technique was done according to Kowalczyk et al. (2011), based on centrifugation. Briefly, samples were centrifuged at 1400 rpm for 10 min at a temperature of 4 °C, followed by pellet re-suspension in deionised water to remove *B. vulgaris* debris and EPS. The supernatant was discarded and pellet dried at 60 °C for 24 h. The dried pellet was then used for characterisation.

The characterisation process included the utilisation of FTIR, PXRD, TEM and SEM-EDS techniques. FTIR was used to determine the reducing mechanism between betanin and metals in *B. vulgaris* solution. The dispersion of the nanoparticles in colloidal suspension was determined using UV-Vis radiation in the range of 200 to 800 nm and the absorption spectrum, including peaks, was monitored. Powder X-ray diffraction was used to determine the crystalline properties of the particles. The size and shape of the nanoparticles were determined using TEM, which were further confirmed by SEM-EDS, which also aided with the elemental analysis.

3.2 Production of biosurfactant

3.2.1 Microorganism used

Bacillus licheniformis STK 01 (accession number: KR01152) is a biosurfactant producing strain isolated from decaying wood (Amodu et al., 2014). The organism was obtained from our culture collection preserved in 80% glycerol stocks and stored at -80 °C. The microorganism was revived by transferring the culture to a sterile nutrient broth subsequent to streaking in nutrient agar plates, and thereafter, incubation at 37 °C for 24 h.

3.2.2 Biochemical analysis of *Bacillus licheniformis* STK 01

The biochemical analysis of the organism was achieved using a Vitek® 2 system (bioMérieux, United States of America). Prior to the Vitek analysis, pure cultures were prepared by re-streaking into blood agar plates followed by incubation between 35 ˚C and 37 ˚C for 18 to 24 h, according to good laboratory practices. With a sterile swab, sufficient numbers of morphologically similar colonies were transferred to a pre-dispensed saline tube. The homogeneous organism suspension was prepared with a density equivalent to the recommended McFarland standard. The solution density was checked using the Vitek 2 DensiCHECK™.

3.2.3 Media preparation and culture conditions for biosurfactant production

Biosurfactant production by *Bacillus licheniformis* STK 01 was enhanced by growing the organism on *B. vulgaris* extract containing different quantities of nanoparticle solutions (Table 3.2). Fermentation was carried out at the organism's optimum conditions: temperature of 30 ˚C and a pH of 7, with an incubator shaking speed of 150 rpm. Biosurfactant production was assessed under both aerobic and anaerobic conditions. To create an anaerobic system, dissolved oxygen in the medium was displaced by pumping nitrogen gas through the medium, and the experiment was thereafter conducted in airtight multiport shake flasks. This was done to prevent the entrance of O_2 into the flasks, which would create a micro-aerobic condition. Samples were taken at 7 h intervals for further analyses. All experiments were carried out in duplicate and respective uninoculated flasks served as controls for each run.

Table 3.2: Processing conditions for biosurfactant production

Method	Run	*BV:* NP ratio	Conditions
A	M1	1:0	Aerobic
	M2	0:1	
	M3	3:1	
	M4	1:3	
	M5	1:1	
B	M1	1:0	Anaerobic
	M2	3:1	
	M3	1:1	
C	M1	FB	Aerobic and
	M2	FB	anaerobic
	M3	FB	

Fed Batch (FB): 2 ml of nanoparticle solution were supplemented at a 7 h interval

BV: *Beta vulgaris* **NP**: Nanoparticles

3.2.3.1 pH and redox potential measurements

The pH and redox potential were measured using a Crison Basic 20 pH meter. The electrode was calibrated before use using Crison buffer solutions (pH 4.00, 7.00 and 9.00). For redox potential the electrode was calibrated using a TISAB solution with known redox potential of 241 mV (See chemical composition in Appendix A1.1).

3.2.3.2 Dissolved oxygen and reducing sugar detection

Dissolved oxygen was measured using an 820 portable dissolved oxygen meter (BANTE820 portable dissolved oxygen meter, BANTE instruments, China). The meter was calibrated between two points, at 0% O_2 in an anoxic solution (see chemical composition in Appendix A1.2) and in 21% O_2 by holding the electrode in an aerated water calibration vessel. Reducing sugars were quantified using a 3,5-dinitrosalicylic acid method (Miller, 1959).

3.2.3.3 Optical density, growth rates and reaction rate kinetics

Bacterial growth was monitored by measuring the optical density of the media using the Jenway 6715 UV/vis spectrophotometer at a wavelength of 600 nm. It was assumed that the organisms' growth rates followed first-order kinetics. Specific growth was calculated using Equation 3.1.

$$\mu = \frac{\ln(X_2 - X_1)}{t_2 - t_1} \quad , \qquad (3.1)$$

where:

μ is the specific growth rate constant (h^{-1}),

X_2 and X_1 are the cell concentration at times t_1 and t_2, respectively.

3.2.4 Biosurfactant extraction and partial purification

The acid precipitation method, as previously described by Joshi et al. (2015) was used for extraction and partial purification of the biosurfactant, with minor modifications in terms of time and speed. Cell-free broth was obtained by centrifugation at 11 000 rpm for 10 min. The pH of the cell-free broth was adjusted to 2.0 using 6 M HCl and incubated at 4 °C for 24 h. Upon incubation, the broth was centrifuged again at 11 000 g for 10 min. The pellet was dissolved in alkaline Milli-Q water and left to evaporate at 60 ˚C overnight in an oven. The biosurfactant was quantified on a dry weight basis. The dried pellet was weighed and reported as gram dry weight per litre (gdw/L).

3.2.5 Biosurfactant activity: Emulsification of hydrocarbon

A volume of 5 mL of kerosene hydrocarbon was added to 5 mL of cell-free supernatant containing the biosurfactant produced by *Bacillus licheniformis* STK 01 using *B. vulgaris* media supplemented with nanoparticles in a graduated 15 mL centrifuge tube. The mixture was mixed using a vortex for 5 min and left to stand for 24 h. The emulsification index was calculated using Equation 3.2.

$$E_{24} = \frac{\text{Total volume of the emulsion}}{\text{Total volume of the aqueous solution+emulsion}} \times 100 \qquad (3.2)$$

CHAPTER 4
RESULTS AND DISCUSSION

4.1 Synthesis of biocompatible metallic nanoparticles from *B. vulgaris*

4.1.1 Introduction

The ideal particle size and unique properties of biocompatible nanoparticles have been of great research interest mainly for their applications in environmental remediation. However, the synthesis of nanoparticles has been a serious challenge, thus the need to produce biocompatible nanoparticles using a completely green chemistry production method. A new method for the green synthesis of biocompatible metallic nanoparticles using plant and agrowaste extracts was developed. *B. vulgaris* was solely used in a synthetic chemical-free redox reaction as a source of precursor metal, reducing and capping agent. Metals hyper-accumulated by *B. vulgaris* plants are reduced to nano size by betanin, an anthocyanin present in the *B. vulgaris* plant extract with remarkable reducing and stabilising capabilities. This polyphenol chelated and reduced the metal ions into nanoparticles.

4.1.2 Aim and objectives

The aims and objectives were to:

- optimise pH and temperatures for the synthesis of biocompatible metallic nanoparticles from *B. vulgaris* agrowaste, and
- Characterise the synthesised nanoparticles using spectroscopic techniques and electron microscopy.

4.1.3 Results and discussion

4.1.3.1 Green method development for synthesis of metallic nanoparticles

Metallic biocompatible nanoparticles were synthesised in a redox chemical-free reaction, using a completely green chemistry method. This was done to pursue the growing interest in developing environmentally safe, inexpensive and efficient methods for synthesis of metallic nanoparticles. In this study, *B. vulgaris* agrowaste material was used for the synthesis of nanoparticles. The use of plant extracts for the synthesis of nanoparticles has been recently and actively pursued as an alternative method for the synthesis of nanoparticles with specified properties and constituents present in tubers. *B. vulgaris* agrowaste was used solely because of its properties. It is a rich source of calcium and phosphorus (Shyamala & Jamuna, 2010) and other valuable compounds such as betanin and anthocyanin, responsible for the red-purple colour of *B. vulgaris.* The anthocyanin has been reported to possess reducing and stabilising properties (Parameshwaran et al., 2013), making it an ideal reducing

agent for nanoparticle synthesis. Metals hyperaccumulated in *B. vulgaris* tubers were effectively reduced to nano size.

4.1.3.2 Effect of pH, temperature, extract concentration and biological supplementation

To determine an ideal method, different parameters were assessed and optimised. The first part of the study was to determine the optimum pH and temperature for nanoparticle synthesis. A *B. vulgaris* solution was used to effectively determine a suitable pH (high/low acidity and high/low alkalinity). To adjust the pH, 1 M HCl and NaOH solutions were used. Temperature was tested at 80 °C and at room temperature (Parameshwaran et al., 2013). Eight samples (1–8), as presented in Table 4.1, were used for the study and monitored for colour change and reaction time. Colorimetric detection for nanopartiles was used to detect the reduction of metals to nano sizes (Kalimuthu et al., 2008; Kowalczyk et al., 2011). During the formation of nanoparticles, a series of colour changes was observed as a result of the betanin which was degraded under different conditions, thus facilitating the reduction of metals to nano size.

Table 4.1: Process parameters and observations for nanoparticle production

Sample ID	pH	Temp ˚C	Supplement	Colour change	Reaction time
1	2	80 ˚C	-	-	-
2	6	80 ˚C	-	-	-
3	8	80 ˚C	-	Purple-red to dark brown	90 min
4	10	80 ˚C	-	Purple-red to dark red	90 min
5	2	RT	-	-	
6	6	RT	-	-	
7	8	RT	-	Purple-red to brown-red	72 h
8	10	RT	-	-	-
9	8	80 ˚C	*A. vera* and eggshell extract	Purple-red to dark brown	90 min
10	8	80 ˚C	-	Red – bright yellow	90 min

RT: Room temperature

There was no significant colour change observed in Samples 1, 2, 5, 6 and 8. This indicated that no chemical reaction took place in these samples. This can be attributed to the pH and temperatures of this samples. The pH normally determines the stability of betanin, which was previously reported to be stable at a pH range of 3–7 (De Azeredo et al., 2009). At this pH range, betanin loses its ability to bind and reduce metal ions which effectively reduces the synthesis of nanoparticles and thus yield. For samples 3, 4, and 7, a chemical reaction was observed by a significant colour change in the samples. In Sample 3 and 7 (refer to Table 4.1), with low alkalinity, the colour changed from purple red to a dark-brown colour. Colour change is an indication of betanin degradation, resulting in the formation of a brown colour as

previously determined by De Azeredo et al. (2009). At alkaline pH, betanin contains more negatively charged functional groups to efficiently bind and reduce cations.

Additionally, the brown colour is normally observed in green synthesis of nanoparticles to detect bioreduction of metals using plant extracts (Mubayi & Chatterji, 2012; Usman et al., 2012). The colour changes observed within the samples can be attributed to the slight degradation of betanin within the samples. Different colour changes for nanoparticle synthesis influenced by betanin from *B. vulgaris* at different pH and temperatures were noted in a study conducted by Parameshwaran et al. (2013). This reaffirmed that pH affects the stability of betanin catalysis which promotes subsequent bioreduction of the metal ions.

Similarly, elevated temperature promotes betanin degradation and subsequent formation of nanoparticles. Samples 5–8 were incubated at room temperature under natural light to promote photocatalytic degradation of the betanin. No colour change was observed in Samples 5, 6 and 8. However, a slow colorimetric reaction was observed in Sample 7, for which the colour changed from purple-red to dark brown after 72 h. This suggested the slow photocatalytic degradation of betanin, as the stability of betanin can also be impaired by natural light (De Azeredo et al., 2009). The degradation of betanin in Sample 7 was also enhanced by the alkalinity of the medium compared with sample 5 and 6.. At elevated temperatures, betanin takes various paths of degradation. It can either be degraded by isomeration, decarboxylation or cleavage (Reshmi et al., 2012). During the formation of nanoparticles, elevated temperatures enhance the synthesis process by increasing the nucleation rate (De Azeredo et al., 2009); thus elevated temperatures were observed to increase the reaction rates compared with lower temperatures.

To confirm nanoparticle production, TEM was used to characterise the size of the particles (Figure 4-1). SEM-EDS was also used to confirm particle shape and to determine particle composition by performing elemental analysis aided by EDS (Figure 4-2). Electron microscope analysis was only carried out on samples that showed a positive chemical reaction (Samples 3, 4 and 7). A freshly prepared and untreated *B. vulgaris* solution was used as a control. For TEM analysis, copper grids were coated with a few drops of the samples by using a Pasteur pipette and were dried under a lamp. The grids were also used for SEM-EDS analysis.

The images obtained from the TEM were examined and confirmed the synthesis of nanoparticles. The control showed irregular structures with sizes of 200 nm (Figure 4-1A). SEM images of control samples revealed what seemed to be biological debris (Figure 4-2A). Sample 3 resulted in well-defined nanoparticles containing spherical-shaped particles of

46.55 nm, with the particle being encapped within a clear capping agent demostrating betanin's reducing and capping capabilities (Figure 4-1B).

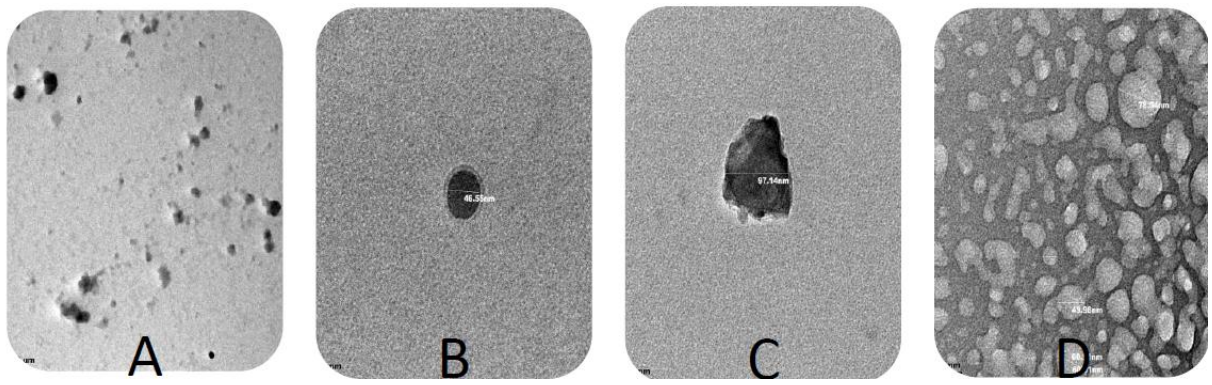

Figure 4-1: TEM images for nanoparticles synthesised

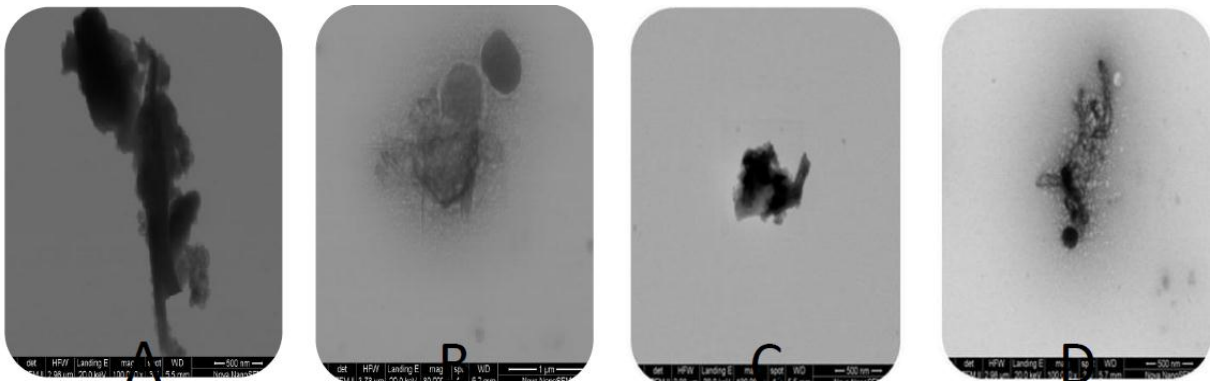

Figure 4-2: SEM images of nanoparticles synthesised

SEM-EDS analysis confirmed spherical shape structures of the particle (Figure 4-2B). Elemental analysis suggested Ca^{2+} was the major constituient (see EDS spectrum in Appendix C1). Sample 4 results showed an irregular shaped crystal-like structure which falls within the nano-size range (Figure 4-1C and 4-2C). No metals were detected from the EDS spectrum of the irregular shaped non-crystal-like structures of Sample 7 (Figure 4-1D and Appendix C2). Al and Si were also detected, presumably as a result of embeded Al and Si assumed to be from the soil (refer to Appendix C1 and C2). On comparing Sample 7 TEM images to those of Sample 3 (Figure 4-1 B and D), the dark shade of the partices was a result of diffracted light by the crystalline structure of the particles.

The light structures observed in TEM images of Sample 7 (Figure 4-1D) showed that the particles were perhaps, non-crystalline. Moreover, crystal particles are formed at high temperatures compared with room temperatures (Makarov, 2014), as observed for Sample 7, which was processed at room temperature (Table 4.1). The successful parameters used for Sample 3 were used for further development of the method. The only limitation of the methods used for the first part of this study was the low yields of the metallic nanoparticles obtained.

4.1.3.3 Improvement of nanoparticle yields using biological agents

In an attempt to improve yields and optimise the in-vitro reaction, biological agents such as *A. vera* were used as supplements. Equivalent quantities of the *B. vulgaris* solution and the *A. vera* were added and incubated at 80 ˚C at pH 8 for Sample 9. For a sustainable greener method, $CaCO_3$ from eggshell extracts was used to adjust the pH and as a supplementary source of Ca^{2+}. Eggshells have been reported to be a rich source of minerallised $CaCO_3$, comprising 94% of the eggshells (Murakami et al., 2007). The colour change and reaction rate of these samples were similar to those of Sample 3. Therefore, *A. vera* had no significant impact on the nanoparticle synthesis reaction rate. However, TEM images (Figure 4-3) revealed a decrease in nanoparticle size and increased particle yields for samples supplemented with *A. vera*. This was aided by the bioactive phytochemicals in *A. vera*.

The particles synthesised in Sample 9 were spherical with a size of less than 10 nm. Moreover, *A. vera* exhibited capping properties, with the nanoparticles synthesised being closely aggregated and encapsulated within the *A. vera* capping agent. The yield and distribution of the nanoparticles in samples supplemented with *A. vera* demonstrated an improvement in comparison with those without *A. vera*.

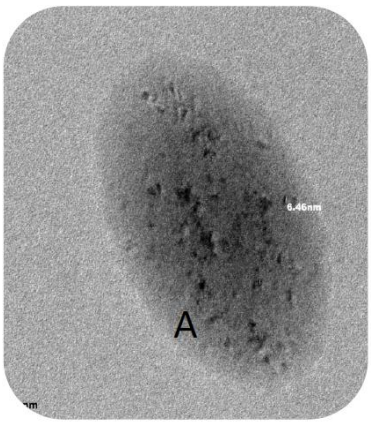

Figure 4-3: TEM image of the sample supplemented with *A. vera*

4.1.3.4 *B. vulgaris* concentration optimisation for nanoparticle production

Previous studies have shown that the quantity of the plant extract required during green synthesis of nanoparticles plays a significant role in nanoparticle formation (Gan et al., 2012; Mubayi & Chatterji, 2012; Parameshwaran et al., 2013). In this study, *B. vulgaris* extract solutions were compared with different concentrations of fresh *B. vulgaris* juice (Table 3.1, Sample 10 to 13). Sample 3 (Table 3.1), containing *B. vulgaris* extract solution, was used for comparison purposes because of the well-defined nanoparticles obtained. The fresh juice extract was used within 48 h of extraction to prevent the solution becoming viscous as a result of moisture loss.

B. vulgaris solutions, 10% (v/v), 1% (v/v), and 0.5% (v/v) (Table 3.1) were used. The latter samples were processed with parameters used successfully in Sample 3 for nanoparticle synthesis as depicted in Figure 4-4, for which a series of colour changes among the samples was observed.

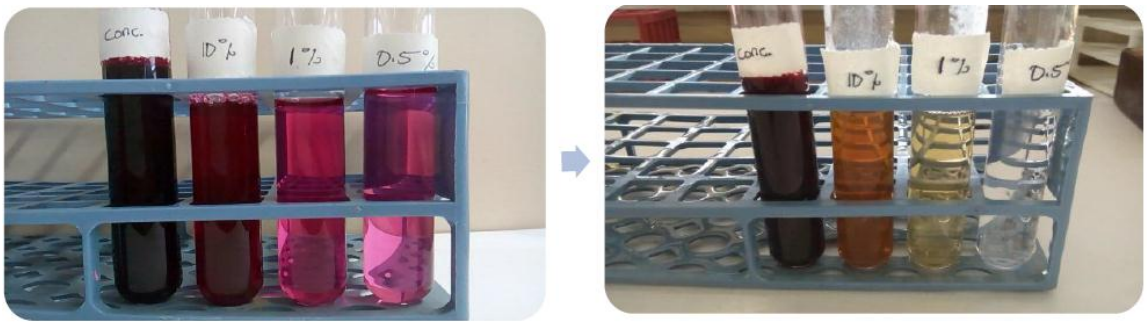

Figure 4-4: A series of colour changes for different concentrations of *B. vulgaris* juice extract

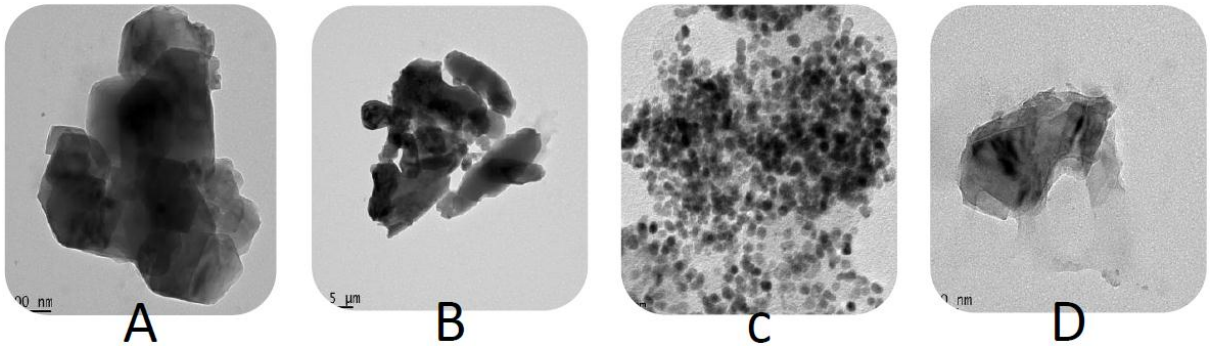

Figure 4-5: TEM images for different concentrations of *B. vulgaris* juice extract used

A slight colorimetric reaction of the concentrated sample (labelled *conc.* in Figure 4.4) changed from a dark-purple colour to a dark-red colour. TEM analysis revealed large crystal-like particles (Figure 4-5A) which were closely aggregated and the particle size was above 200 nm, which was above the nanoparticle size range. A series of colour changes was observed for samples in which *B.vulgaris* concentrations were 10% (v/v), 1% (v/v) and 0.5% (v/v). The samples in which the *B. vulgaris* concentration was 10% (v/v), had a colour change that resulted in a brown colour from a red colour, resulting in large rod-like structures of 200 nm in size (Figure 4-5B).

It was important to note that the *B. vulgaris* juice concentration determined the shape of the particles being formed. However, higher concentrations resulted in larger particle sizes. Moreover, low concentrations such as 0.5% (v/v) resulted in what seemed to be biological debris (Figure 4-5D). An ideal colour change was observed in samples with a low *B. vulgaris* 1% (v/v) solution, for which the colour changed from pink to a bright yellow colour. This colour change indicated the presence of neobetanin.

Neobetanin is an isomer of betanin that results in the dehydrogenation of the betanin which generates a bright yellow colour. This hydrolytic cleavage of hydrogen ions is also promoted by an alkaline pH, which in turn determines neobetanin's ability to bind and reduce metal ions during nanoparticle formation. The 1% (v/v) *B. vulgaris* solution samples (Sample 10 in Table 4.1), showed riveting TEM images (Figure 4-5C). The TEM results showed higher yields and improved distribution of spherical-shaped nanoparticles confirmed by SEM (Figure 4-6) with a size of approximetly 10 nm.

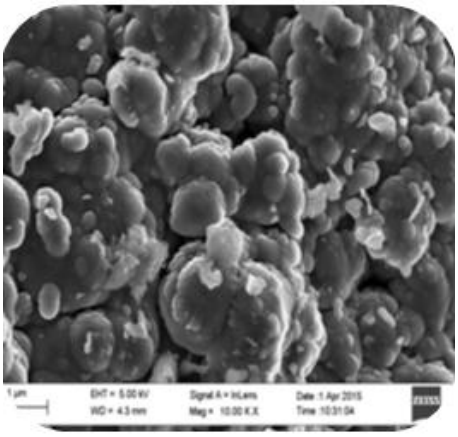

Figure 4-6: SEM image of Sample 10

EDS spectrum (Figure 4-7) of the aqueous solution of Sample 10 suggested that calcium ions (Ca^{2+}) were the major constituent in the solution. The absence of O_2 from the spectrum is attributed to the fact that the nanoparticles were not oxidised. Therefore, this meant that Ca-based nanoparticles synthesised from Sample 10 included other metals such as Cu and P in very small quantities. The yield and distribution of the nanoparticles for Sample 10 improved significantly compared with Sample 3 and 9 (Figure 4-1B and 4-3). The well-defined nanoparticles obtained in Sample 10 were used for further characterisation.

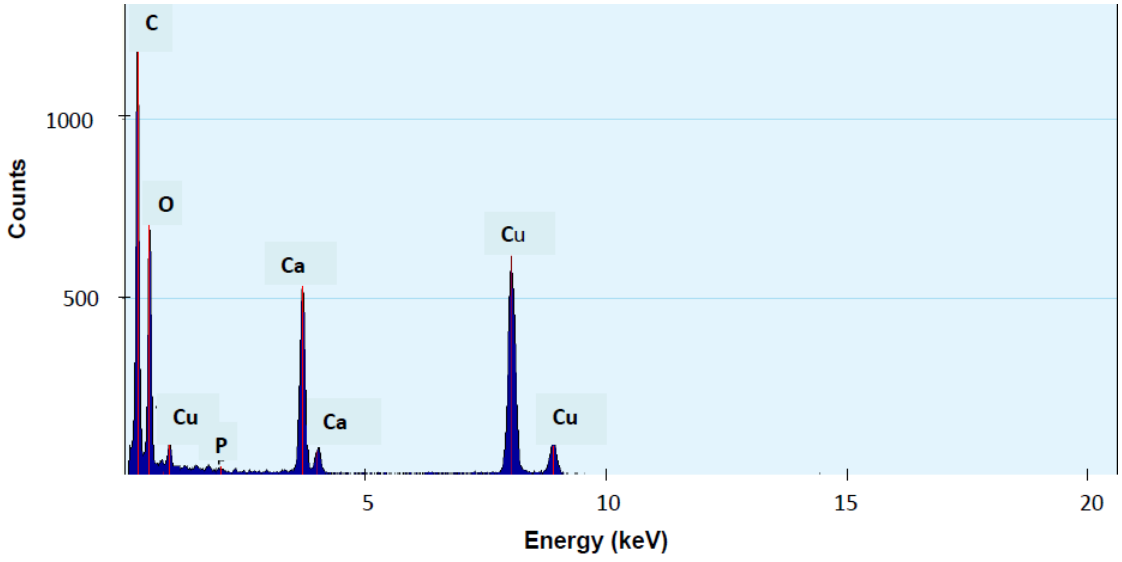

Figure 4-7: EDS spectrum of Sample 10

4.1.3.5 Spectrophotomeric characterisation of nanoparticles

UV-Vis spectroscopy was used to establish the stability of the metallic nanoparticles in an aqueous solution. Figure 4-8 illustrates the absorbance spectra of the nanoparticles synthesised from the 1% (v/v) solution of *B. vulgaris* juice extract (Sample 10). The UV-Vis spectroscopy of the nanoparticle aqueous solution showed absorbance at a wavelength of 418 nm. The bright yellow colour of the aqueous solution was hypothesised to be the surface plasmon of the nanscent nanoparticles. Nanoparticles between the size range of 2 to 100 nm have a strong and broad surface plasmon peak at respective wavelengths. This is because the optical absorption spectra of metallic nanoparticles is influenced by surface plasmon resonances (SPR) which move towards longer wavelengths with increases in particle size (Mubayi & Chatterji, 2012). The UV-Vis spectrum of the aqueous solution presented a single SPR band which disclosed the spherical-shaped characteristics of the nanoparticles. This phenomenon is supported by Mie's theory which briefly states that a single SPR results in spherical-shaped nanoparticles (Link & El-Sayed, 2000). These findings were confirmed by SEM images of Sample 10, which showed the synthesis of spherically shaped nanoparticles (see Figure 4-6).

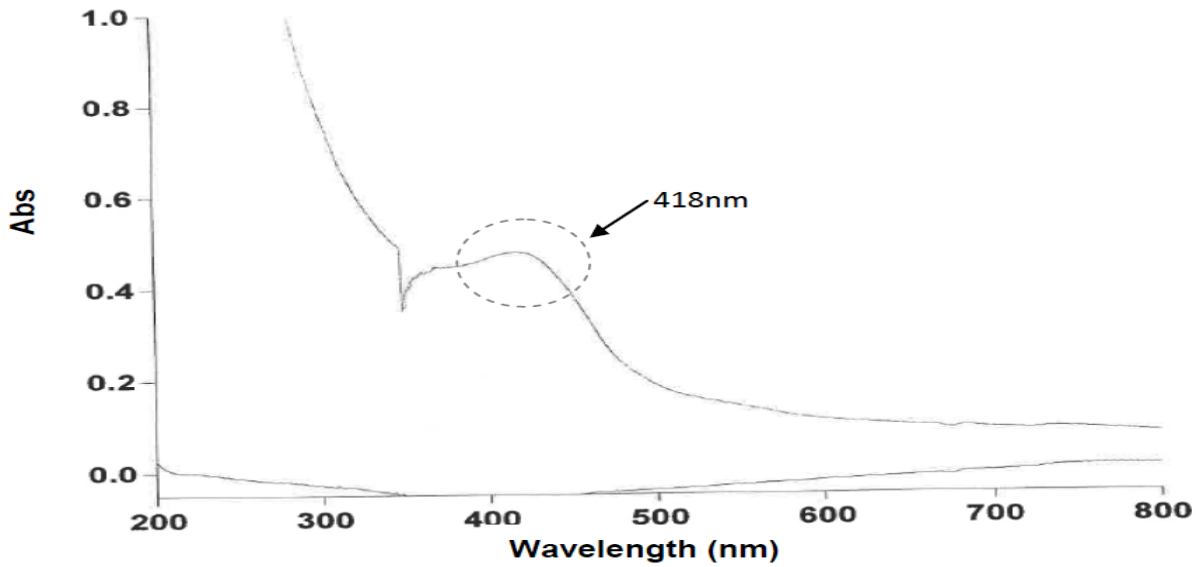

Figure 4-8: UV-Vis spectrum of Sample 10

The crystallisation aspects of the synthesised nanoparticles were analysed using powder X-ray diffraction (PXRD). PXRD is a non-destructive technique that allows analysis of unknown materials in terms of crystallinity and phase identification (Taglieri et al., 2013). The PXRD pattern of the synthesised nanoparticles presented sharp narrow peaks which revealed the formation of crystal nanoparticles. The diffracted peaks originating at the 2 theta degrees illustrated characteristics of calcium line indexed at (001) and (100) with diffraction angles of

18.0 and 28.6, respectively. Therefore, it can be presumed that crystal Ca-based nanoparticles were successfully obtained.

The peaks exhibited in the diffractogram were in accordance with JCDDS file 87-0315 of $Ca(OH)_2$ nanoparticles reported by Darroudi et al. (2016). The presence of unidentified peaks in the pattern may be a result of impurities in the sample or crystallised EPS of the plant extract (Usman et al., 2012; Parameshwaran et al., 2013).

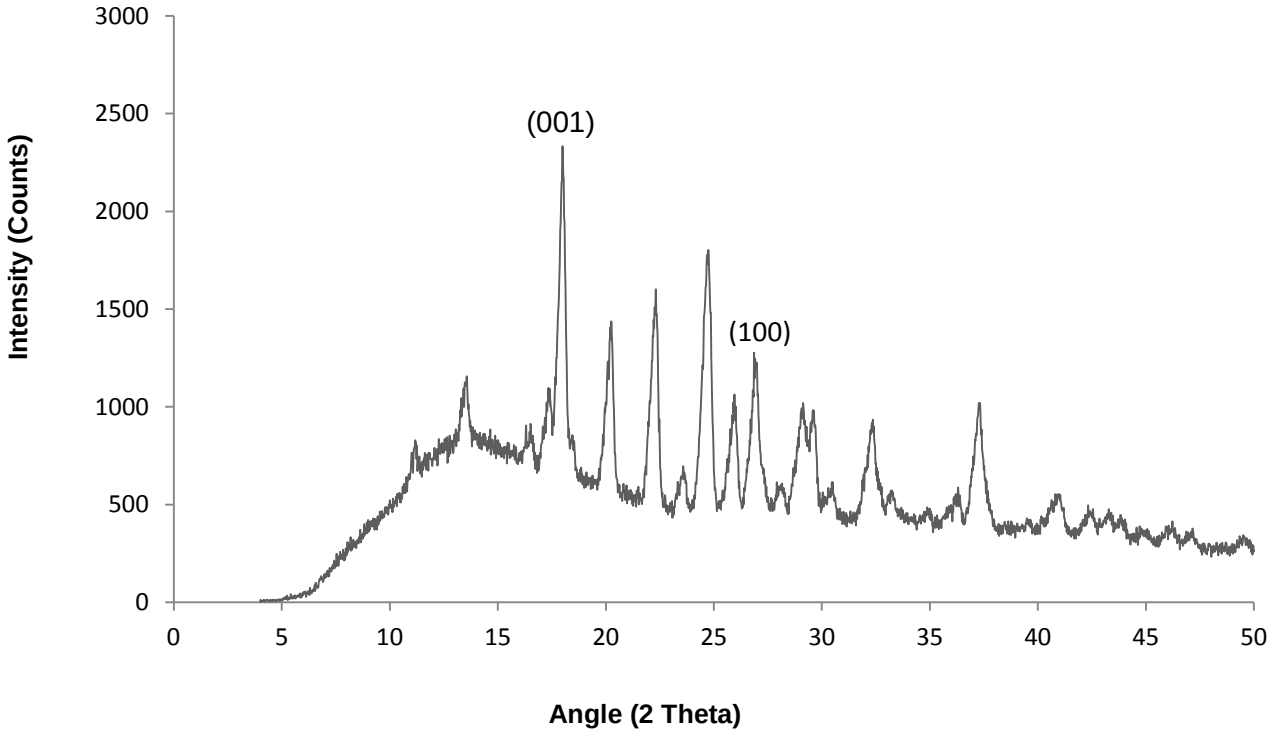

Figure4-9: PXRD pattern of Ca-based nanoparticles obtained from Sample 10

To determine the reduction mechanism of the metals and betanin within the *B. vulgaris*, FTIR analysis was also conducted. The FTIR spectrum of Sample 10 (Figure 4-9) showed transmissions at 3270 cm^{-1}, corresponding to a hydroxyl (OH) vibration band. This suggests that a proton dissociated from the OH group, accompanied by a reduction of metal ions as discussed in Section 2.5.2. From the FTIR spectra, carbonyl groups exhibited a stretching frequency at 1634.03 cm^{-1}. The presence of these molecular groups provides stability and capping of nanscent nanoparticles. This suggests that the nanoparticles were capped by a polymer as seen in Figure 4-1B for Sample 3. The general decrease in the bands observed at 571.87 and 406.09 cm^{-1} indicated metallic nanoparticles formed using betanin. At this point, the functional groups of betanin interacted with the metals found in *B. vulgaris* for the formation of nanoparticles. A similar trend was observed in the FTIR spectrum for betanin, for the analysis of the surface structure of silver nanoparticles (Parameshwaran et al., 2013).

These suggested that there was a reaction between free metal ions and betanin found in *B. vulgaris* for the formation of nanoparticles. From the spectrophotometric findings, Equation 4.1 was hypothesised to be the mechanism of the crystal Ca-based nanoparticle formation.

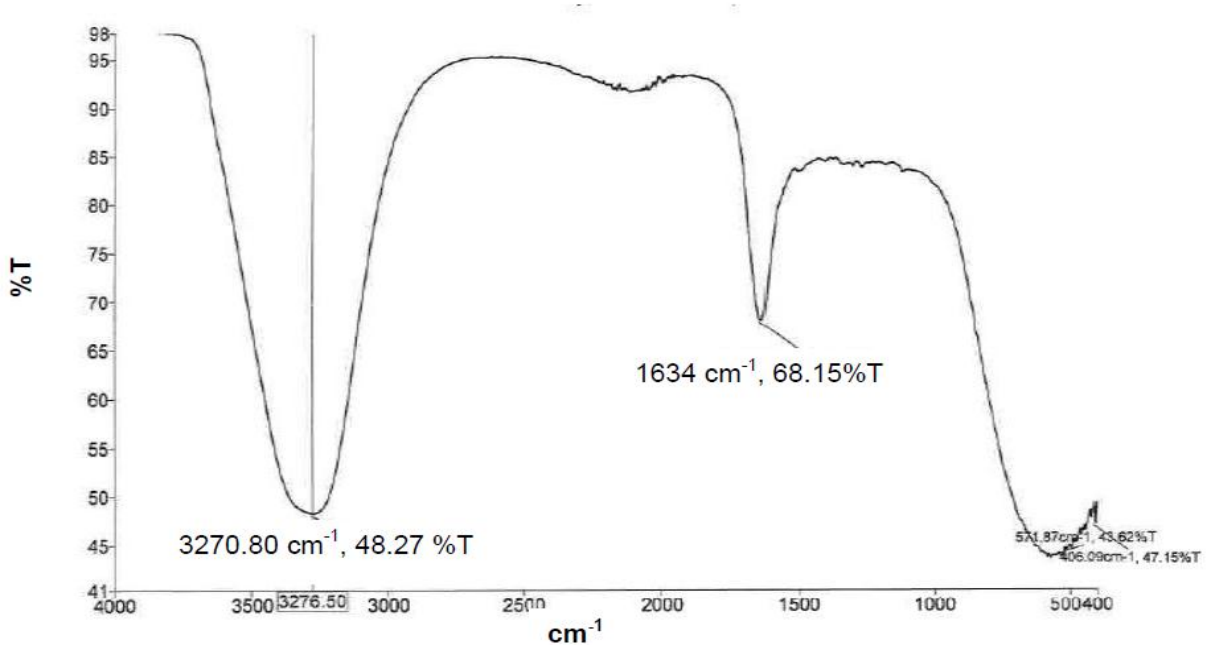

Figure 4-10: FTIR spectrum of Sample 10

The equation 4.1 illustrates the importance of temperature on reaction rates, which would ultimately result in the formation of crystal Ca-based nanoparticles. Elevated temperatures promoted the thermal degradation of betanin, releasing an active hydrogen molecule by dehydration which resulted in the conversion of betanin to neobetainin, and which emitted a bright yellow colour. The released H^+ binds and interacts with metal ions in the solution based on their electrochemical potential as previously explained (Section 2.3.3). In this study, Ca^{2+} ions were determined to be suscetible to reduction. According to Le et al. (2013), the reaction time has a significant impact on particle size and size distribution.

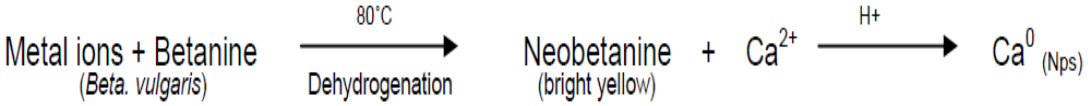

(Equation 4.1)

4.1.4 Summary

B. vulgaris agrowaste and fresh extract were exploited for the synthesis of nanoparticles. Results showed that elevated temperatures resulted in the degradation of betanin within *B. vulgaris* and released an effective proton. The released proton reduced Ca^{2+} ions found in high concentrations within the *B. vulgaris.* Moreover, alkaline pH was determined to also affect the effectiveness of the betanin. At alkaline conditions, the functional groups of the betanin were susceptible to binding and thus reduction. Synthesis of the nanoparticles was proved by a change in colour of the reaction mixture after incubation at 80 °C and pH of 8. Nanoparticles with ideal characteristics were synthesised using a 1% (v/v) *B. vulgaris* solution, for which the reaction mixture changed from a pink to a yellow colour.

This indicated bioreduction of free metal ions and the conversion of betanin to neobetanin. SEM-EDS revealed spherical-shaped Ca-based nanoparticles of approximatly 10 nm determined by TEM. The UV-Vis spectrum of the aqueous solution presented a single SPR band at 418 nm. Powder X-ray diffraction revealed sharp non-broadening peaks, suggesting crystallinity of the particles. FTIR was used to investigate the reduction mechanism of metals by betanin in the *B. vulgaris*. It was determined that hydroxyl groups release an H^+ ion, which subsequently reduces the metals. The findings also showed that the synthesis of nanoparticles can be enhanced using other biological agents such as *A. vera* for smaller sized nanoparticles with improved yields and eggshell extract to adjust pH.

4.2 Enhanced biosurfactant production by *Bacillus licheniformis* STK 01 using Ca-based nanoparticles

4.2.1 Introduction

The crystal Ca-based nanoparticles that were previously synthesised (see Section 4.1), were used to enhance biosurfactant production by *Bacillus licheniformis* STK 01. The influence of Ca-based nanoparticles on the growth rate, yield and other fermentation parameters was closely monitored. Calcium-based nanoparticles such as CaO nanoparticles are known to exhibit unusual catalytic properties and are applicable in diverse fields (Safaei-Ghomi et al., 2013). Recently, CaO nanoparticles have been used to catalyse transesterification of sunfower oil as well as many other chemical transformations (Luz Martínez et al., 2011; Safaei-Ghomi et al., 2013). To the best of the authours knowledge, this study is the first to report Ca-based nanoparticle application in a biochemical process used for the production of biosurfactants for environmental engineering applications.

4.2.2 Aims and objectives

The aims and objectives of this study were to:

- perform a biochemical analysis of the *Bacillus licheniformis* STK01 using a Vitek system,
- enhance biosurfactant production using *B. vulgaris media* supplemented with nanoparticles, and
- investigate biosurfactant activity, by quantifying the emulsification index and the stability of the formed emulsions in comparison with those that were achieved using the same fermenter in a previous study.

4.2.3 Results and discussion

4.2.3.1 Confirmatory tests of biosurfactant-producing *Bacillus* strain

. *Bacillus licheniformis* STK 01 was previously isolated and identified by Amodu et al. (2014), and thereafter crypreserved at -80 °C in 80% glycerol stock. *B. licheniformis* STK 01 was re-activated by inoculating the culture in nutrient broth subsequent to sub-culturing in nutrient agar. Biochemical tests were performed on STK 01 using the VITEK® system (version 07.01). The VITEK® system is an automated system that is based on microbial substrate utilisation and enzymatic reactions (Clontz, 2009). The Vitek results confirmed that the strain used was *Bacillus licheniformis*. The biochemical test results are shown in Table 4.2. The results also revealed that the microorganisms have the ability to produce useful biological products such as hydrolytic enzymes, for example, BXYL codes for β-Xylosidase, an enzyme that hydrolyses xylobiose, a disaccharide of xylose monomers. Furthermore, positive results emerged for βGAl (α-galactosidase) and α-AGLU (α-galactosidase), two enzymes involved in the hydrolysis of complex carbohydrates releasing, glucose monomers.

These enzymes enable the bacterium to utilise complex carbohydrates most commonly found in agrowastes. Vijayalakshmi et al. (2013) proved that *Bacillus licheniformis* has the ability to utilise lignocellulistic material such as leaf litter biomass, while Van Dyk et al. (2009) reported that the organism has the ability to produce large multi-enzyme complexes. Moreover, the Vitek® results (Table 4.2) revealed that the microorganisms have the ability to produce pheA, TryA and Leu A, enzymes which are responsible for the biosynthesis of amino acids, major contituents in the production of lichenysin, a LMW lipopeptide biosurfactant. Therefore, these results confirm the ability of strain STK 01 to produce a lichenysin biosurfactant.

Table 4.2: *Bacillus licheniformis* STK 01 Vitek biochemical test results

Biochemical test	Result (+/-)	Biochemical tests	Result (+/-)
BXYL	+	**ELLM**	+
LysA	-	**Mdx**	-
AspA	-	**AMAN**	-
PheA	+	**GlyA**	+
ProA	-	**dMAN**	+
βGAl	+	**dMNE**	+
PyrA	+	**dMLZ**	-
AGAL	-	**NAG**	-
TryA	+	**IRHA**	-
BNAG	-	**BGLU**	+
APPA	-	**BMAN**	-
CDEX	+	**PHC**	-
dGAL	-	**PVATE**	+
INO	+	**dTAG**	+
MdG	+	**dTRE**	+
INU	+	**KAN**	+
dGLU	+	**OLD**	+
dRIB	+	**Esc**	+
NaCl 6.5%	+	**TTZ**	+
POLYB-R	+	**α-AGLU**	+

4.2.3.2 Bacterial growth curve and biosurfactant production yield

The enhancement of biosurfactant production by *Bacillus licheniformis* STK01 using Ca-based nanoparticles was assessed under various conditions. The production was performed under aerobic and anaerobic conditions. Different quantities of the nanoparticle solution were added to *B. vulgaris* growth media (see Table 3.2 for media composition) and the production was carried out at the bacterium's optimum temperature of 30 °C and pH of 7. The growth of *Bacillus licheniformis* STK 01 in all the tested media for which fermentation was performed under various conditions, was used to monitor bacterial growth and biosurfactant production yield. The tests were carried out in duplicate and an uninoculated sample served as a control for each run. In this case, Run M1 served as a control where the media contained *B. vulgaris* solution without Ca-based nanoparticles, while all other media contained nanoparticles under both aerobic and anaerobic conditions.

Figure 4-11 shows the growth curve of the bacterium under aerobic conditions. The lag phase in M2, M3 and M5 took up to 7 h and longer, followed by the exponential phase. However, Run M2 had a shorter exponential phase as there was a decrease in microbial growth after 14 h. Run M1 maintained the exponential phase for up to 28 h, with Run M4 obtaining the highest bacterial cell concentration under aerobic conditions.

This demonstrated that Ca-based nanoparticles had a positive impact on the bacterial growth rate. Runs M3 and M5, containing a larger quantity of Ca-based nanoparticles, exhibited a higher growth rate (Table 4.3), while a higher cell concentration was achieved compared with Run M1. Run M2 that contained a higher concentration of the Ca-based nanoparticle solution, showed a lower bacterial growth rate. This could be attributed to minimal or limited carbon source availability in the media and/or the impact of the Ca-based nanoparticles on the organism. Intriguingly, Ismail et al. (2013) reported that ZnO nanoparticles inhibited growth of crude oil utilising bacteria when the nanoparticles were used at higher concentrations. However, in this study, the fermentation results revealed that bacterial growth was favoured in media containing Ca-based nanoparticles than in media without the Ca-based nanoparticles.

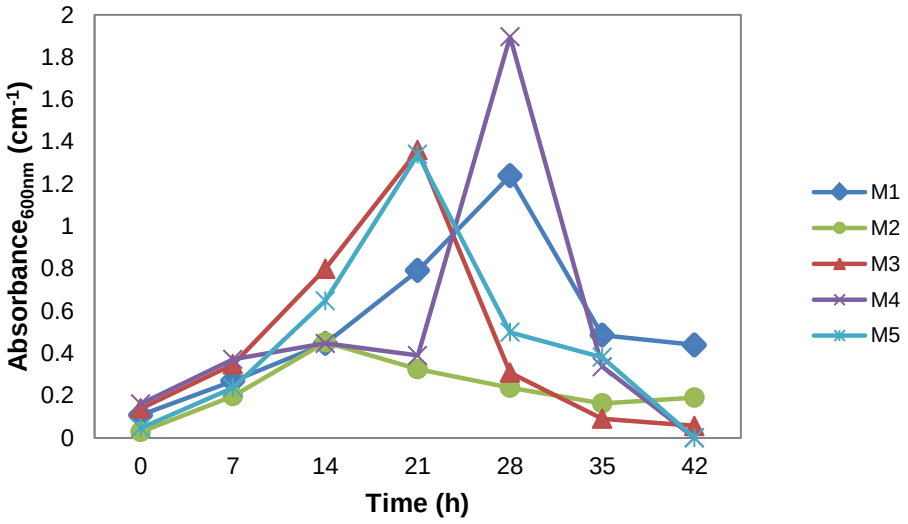

Figure 4-11: *Bacillus licheniformis* STK01's growth in different media under aerobic conditions

After fermentation, the biosurfactant was recovered from a cell-free culture using the acid precipitation method and partial purification. It was determined that minimal biosurfactant yield was observed in media containing large quantities of Ca-based nanoparticles, for example, in Run M2 and M4, a phenomenon which might have reduced the activity of the bacterium. This suggested that large quantities of the Ca-based nanoparticles can have an adverse impact on biosurfactant production or activity. It was paramount to note that Run M4, with the highest bacterial growth concentration, also resulted in minimal biosurfactant production. This is supported by the fact that biosurfactant is a secondary metabolite, that is, it is a non-growth associated metabolite. Therefore, biosurfactant production was observed to be independent of microbial growth. This was also noted with Run M5, in which the highest growth rate of 0.16 h^{-1} and a biosurfactant yield of 0.02 gdw/L were observed. Run M3 had a growth rate of 0.1088 h^{-1} and produced the highest biosurfactant yield under aerobic conditions (see Table 4.3). All nanoparticles containing media had the highest biosurfactant yield compared with Run M1, which was without nanoparticles. This revealed that Ca-based nanoparticles' catalytic properties had enhanced biosurfactant production. Observations from this study also suggested that the quantity of nanoparticles used to enhance biosurfactant production was important

Table 4.3: *Bacillus licheniformis* STK 01's growth rate and biosurfactant production yield under different conditions

Condition	Run	Growth rate (h^{-1})	Partially purified biosurfactant yield (gdw/L)
Aerobic	M1	0.0873	0.01
	M2	0.1159	0
	M3	0.1088	0.05
	M4	0.0882	0
	M5	01600	0.02
Anaerobic	M1	0.1718	0.03
	M2	0.0466	0.04
	M3	0.1732	0.02
Fed-batch Fermenation (Aerobic/Anaerobic)	**M1**	**0.0597**	**0.35**
	M2	**0.0169**	**0.27**

Media that were deemed to be suitable for biosurfactant production under aerobic conditions were also studied under anaerobic conditions. This was done to further evaluate *Bacillus licheniformis* STK 01 performance under anaerobic conditions. As shown in Figure 4-12 and similar to aerobic conditions, the lag phase lasted up to 7 h for all media and thereafter, followed by an exponential growth phase that lasted up to 14 h. For Run M1, the exponential phase lasted for 21 h prior to the death phase, whereas for Run M2 and M3, the exponential growth phase was followed by a stationary phase which lasted up to 21 h. Run M1 without the Ca-based nanoparticles obtained the highest cell concentration compared with the other two media with Ca-based nanaoparticles. Run M2 had a slower growth rate (Table 4.3) compared with all other media, both under aerobic and anaerobic conditions.

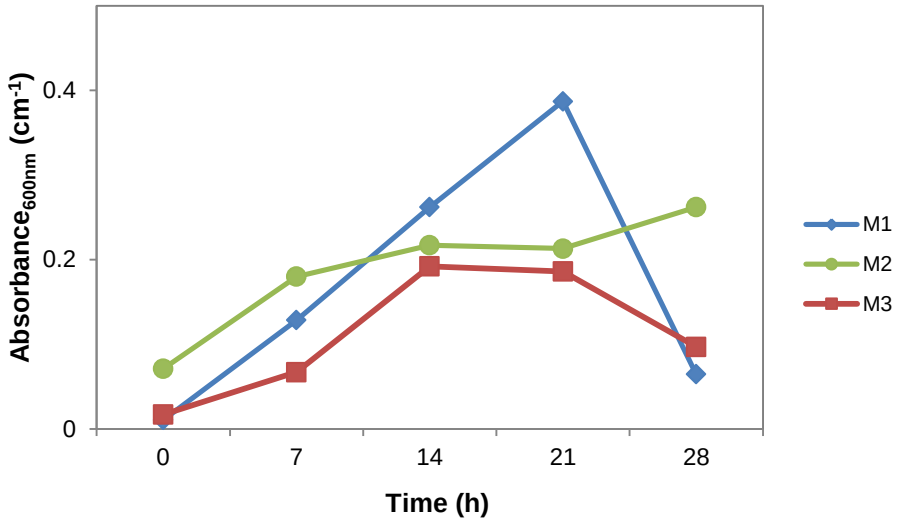

Figure 4-12: *Bacillus licheniformis* STK 01's growth under anaerobic conditions

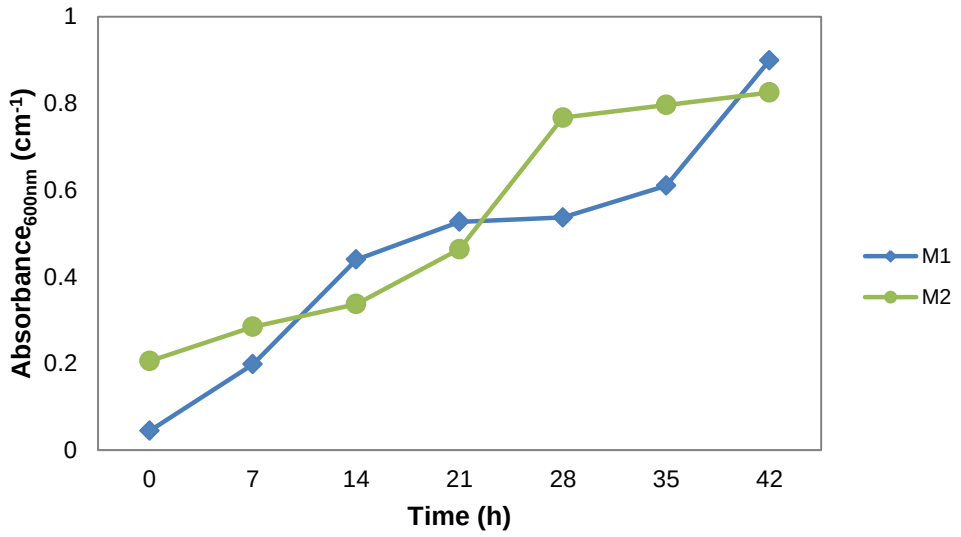

Figure 4-13: *Bacillus licheniformis* STK 01's growth in fed-batch fermentation for both aerobic and anaerobic conditions

Foam formation during fermentation occurred as a result of active microbial products such as the biosurfactant, and the resultant foam is considered undesirable. It was therefore used as a qualitative measure for biosurfactant production, with stable form formation being observed in other media when the flasks were hand shaken. However, despite the excessive foam formation for Run M2 samples, the highest biosurfactant yield of 0.04 gdw/L under anaerobic conditions was observed. Run M3 had the highest growth rate with the lowest biosurfactant yields. Run M3 under anaerobic conditions and Run M5 under aerobic conditions had similar media compositions (Table 3.2) and produced an equivalent quantity of biosurfactants (Table 4.3). This demonstrated that the organisms' dissolved oxygen requirements had minimal or no impact on biosurfactant production.

Ca-based nanoparticle-containing media showed enhanced biosurfactant production yields compared with non Ca-based nanoparticle cultures. In an attempt to improve yields in nanoparticle-containing media, a fed-batch fermentation was carried out at both aerobic and anaerobic conditions. Fermentation was carried out for a period of 42 h. A 5 mL solution of nanoparticles was supplemented at a 7 h interval in fermentation containing solely *B. vulgaris* extract growth media. *Bacillus licheniformis* STK 01 (M1) demonstrated continuous growth for up to 42 h using the fed-batch system. Run M2 experiments tested under anaerobic conditions showed maximum growth. However, Run M1 tested under aerobic conditions had the highest yield of 0.35 gdw/L compared with experiments carried out in this study (Table 4.3). Therefore, this study demonstrated that Ca-based nanoparticles enhanced biosurfactant production when *B. vulgaris* was used as a substrate.

4.2.3.3 Effect of temperature, pH, redox potential (mV), dissolved oxygen and carbon source

Physicochemical conditions such as temperature, pH, and redox potential have a significant influence on microbial growth and product formation. The temperature was maintained constant throughout the fermentation period. In a fermentation process, temperature is considered a rate-limiting step. Higher temperatures increase bioreaction rates and this can decrease product formation. However, optimum temperature promotes cell performance and microbial growth, as well as product formation.

The pH of a fermentation system also influences microbial growth. *Bacillus licheniformis* STK 01 under aerobic and anaerobic fermentation, and in fed-batch fermentations, showed significant fluctuations (Figure 4-14; 4-15 and 4-16). For aerobic conditions (Figure 4-14), minor fluctuations were observed for media with the highest growth (Run M4). The pH was slightly maintained close to neutral pH values. For the duration of the fermentation, media with the highest production yield (Run M3) were maintained at a constant pH. This was supported by the findings reported by Dadrasnia and Ismail (2015), using a *Bacillus* sp. for which the highest biosurfactant yield was observed at pH between 5 and 9. For anaerobic cultures (Figure 4-15), the pH of the medium showed a significant decrease during the lag phase. After 21 h, the bacterium reached the death phase, resulting in pH increases. This was assumed to be a result of *Bacillus licheniformis* STK 01 cell lysis which resulted in the release of intracellular pH increasing microbial constituents. For the fed-batch cultures (Figure 4-16) under anaerobic conditions (Run M2), the pH was at low acidic levels, whereas for the fed-batch cultures under aerobic conditions (Run M1), the pH fluctuated throughout the fermentation period. This showed that *Bacillus licheniformis* STK 01 has the ability to withstand unfavourable and harsh conditions of the surrounding environment.

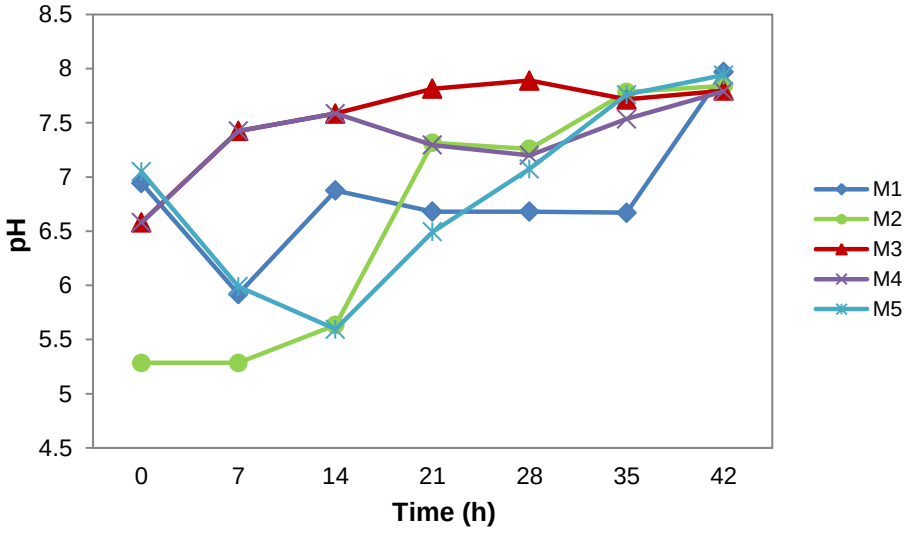

Figure 4-14: pH for biosurfactant production media under aerobic conditions

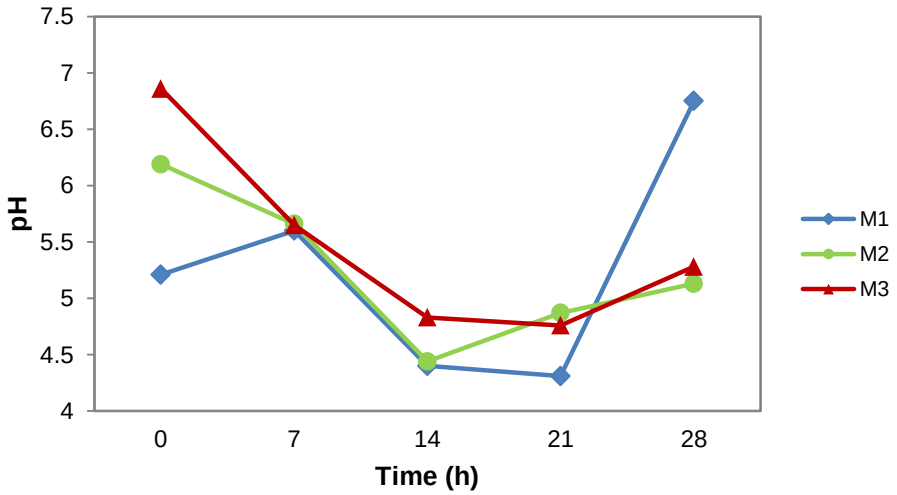

Figure 4-15: pH for biosurfactant production media under anaerobic conditions

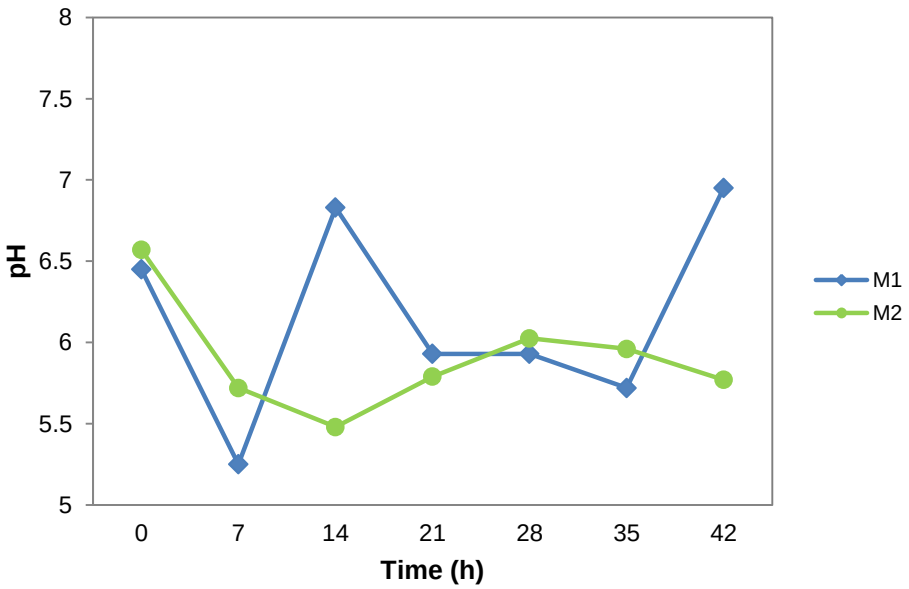

Figure 4-16: pH for biosurfactant production media in fed-batch fermentations under aerobic (Run M1) and anaerobic (Run M2) conditions

Another important parameter that was monitored was the redox potential (Figure 4-17, 4-18 and 4-19). The redox potential was found to be inversely proportional to the pH in all media used under different fermentation conditions.

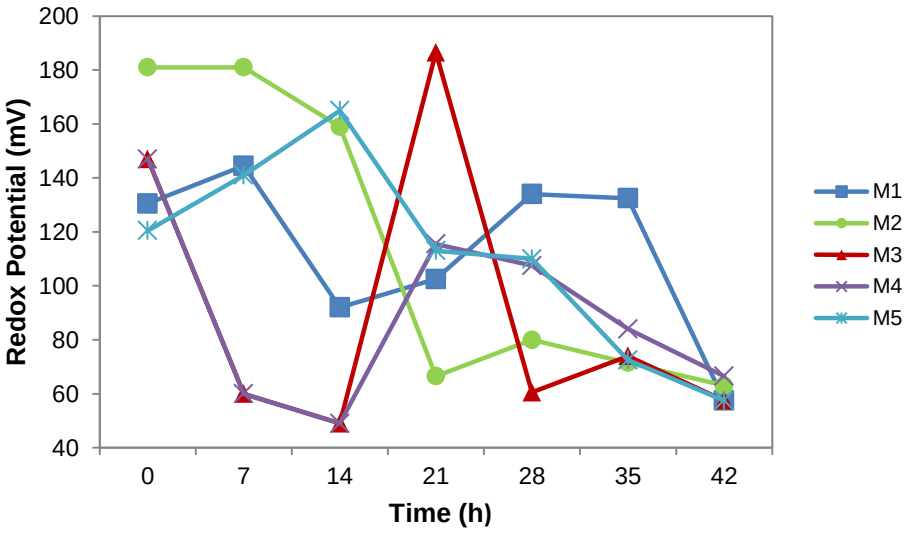

Figure 4-17: Redox potential (mV) for biosurfactant production media under aerobic conditions

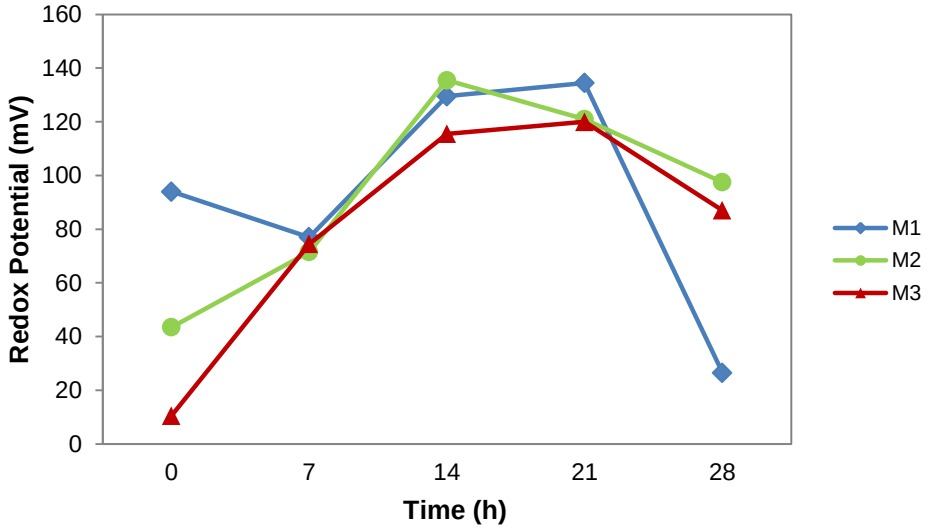

Figure 4-18: Redox potential (mV) for biosurfactant production media under anaerobic conditions

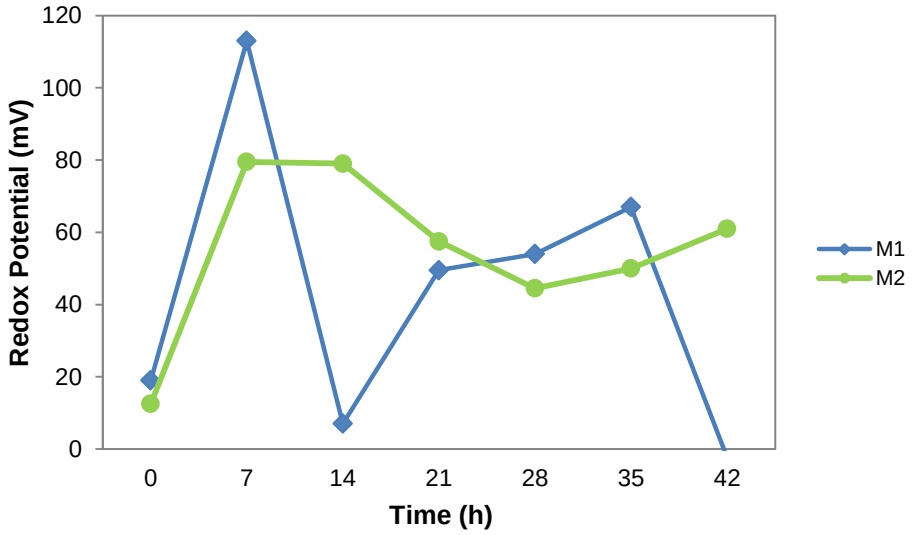

Figure 4-19: pH for biosurfactant production media in fed-batch fermentation under aerobic (Run M1) anaerobic (Run M2) conditions

The redox potential (mV) influences the rate and extent of the bacterium's redox reactions. This means that it can have a significant impact on bacterial growth and product formation. Redox potential is a collaborational function of other environmental parameters such as pH and DO. DO was also another important parameter to monitor in the aerobic fermentations. For aerobic fermentations, the dissolved oxygen was measured prior to sampling. The dissolved oxygen was maintained around 6 mg/L (Figure 4-20). A decrease was observed at 14 h when microbial growth was in the exponential phase. This indicted that the rate of oxygen consumption exceeded the rate of oxygen supply.

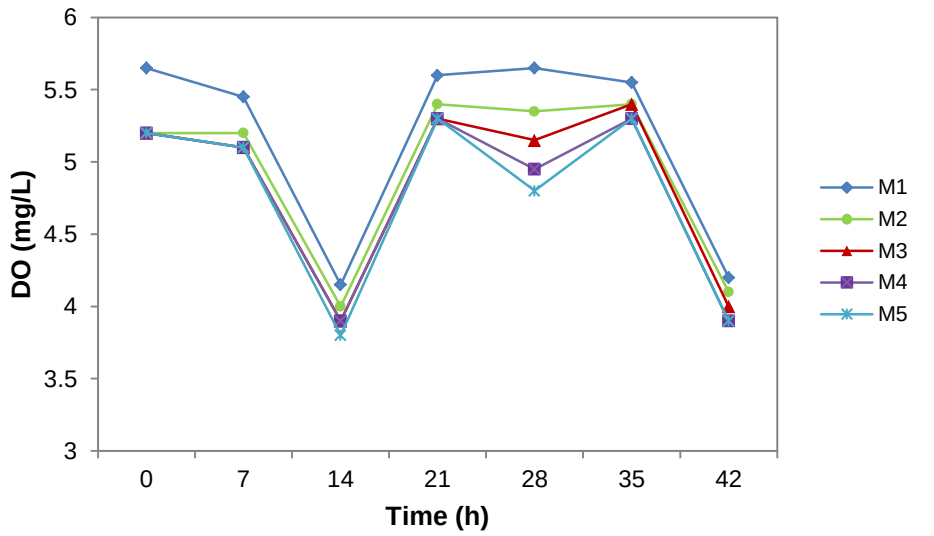

Figure 4-20: DO for biosurfactant production media under aerobic conditions

In this study, *B. vulgaris* was used as a sole carbon, nitrogen and trace element source for biosurfactant production. Utilisation of *B. vulgaris* by *Bacillus licheniformis* STK01 was monitored by measuring reducing sugars in the fermentation media. During fermentation, reducing sugars are gradually released from the lignocellulistic material into the medium. Figure 4-21, 4-22 and 4-23 showed that Run M1, under all assessed conditions, had the highest concentration of reducing sugars released. Results also showed that media containing Ca-based nanoparticles had the lowest reducing sugar concentrations. This indicated that in these media, the carbon source was the rate-limiting nutrient. However, it was important to further highlight the fact that the excess carbon source observed in Run M1 resulted in low biosurfactant yield. This was also observed in a study conducted by Attia et al. (2013), in which increased olive oil concentration decreased biosurfactant production by *Nocardia amarae*. Therefore, these findings suggested that the biosurfactant production was not carbon source dependent. This study also showed that Ca-based nanoparticles containing media with limited carbon source produced a high yield of biosurfactant.

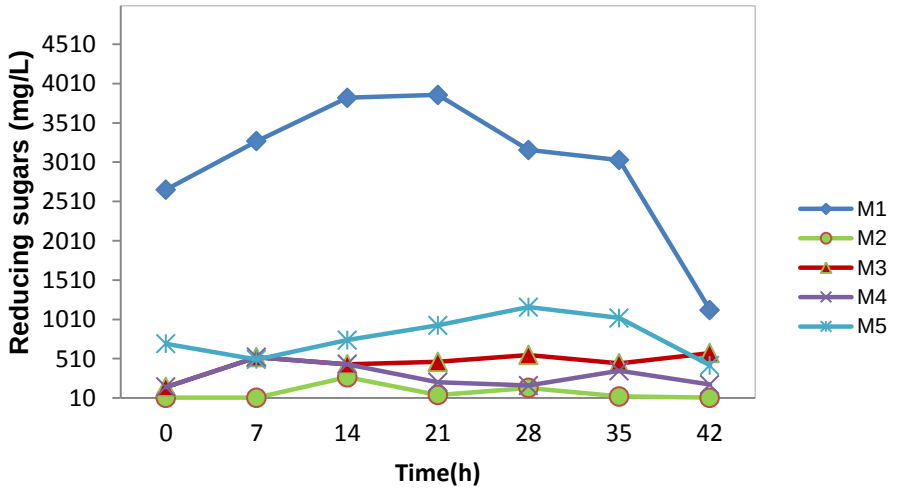

Figure 4-21: Reducing sugar profile under aerobic conditions

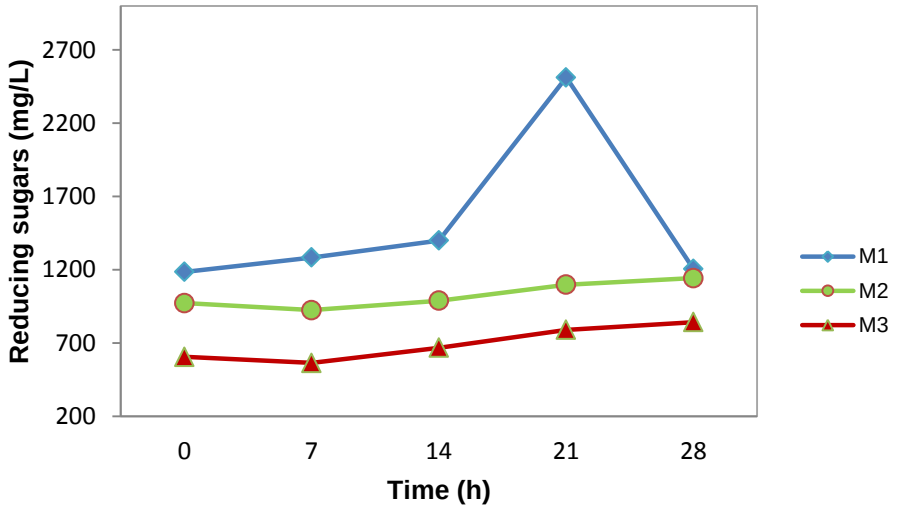

Figure 4-22: Reducing sugar profile under anaerobic conditions

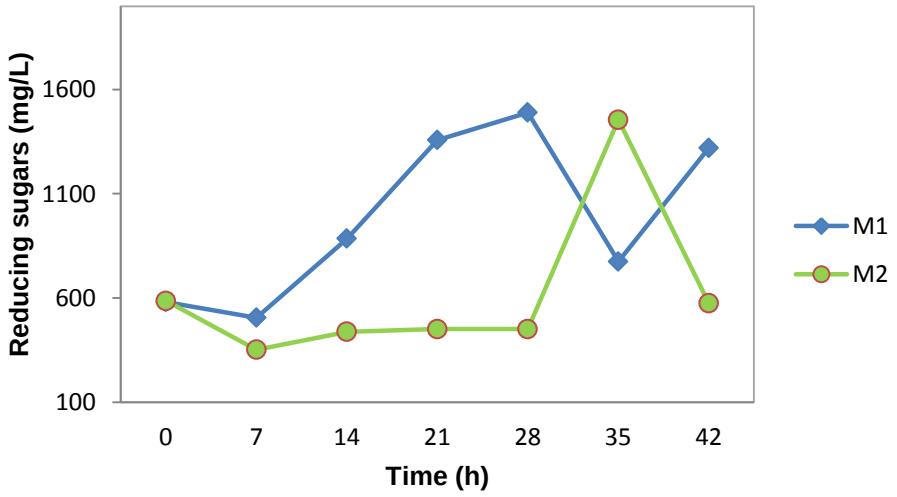

Figure 4-23: Reducing sugar profile in a fed-batch mode under aerobic (Run M1) and anaerobic (Run M2) conditions

4.2.3.4 Effiency of enhancing produced biosurfactant in remediating hydrocarbon

The biosurfactant produced in Run M1 in fed-batch fermentations with the highest yield was assesed for hydrocarbon emulsification activity. The ability of the biosurfactant to emulsify hydrocarbons determines its effectiveness in environmental applications for the bioremediation of hydrophobic contaminants (Amodu et al., 2014). In this study, commercial kerosene hydrocarbon was emulsified using the biosurfactant produced by *Bacillus licheniformis* STK 01 in *B. vulgaris* supplemented with Ca-based nanoparticles. Table 4.4 shows emulsification of the kerosene with a biosurfactant produced by *Bacillus licheniformis* STK 01, compared with previous studies. The emulsification index of kerosene in this study was determined to be 50% and stable for over 24 h, compared to a previous study (Amodu et al., 2014) whose efficiency was below of that found in this study

Table 4.4: Emulsification of kerosene by *Bacillus licheniformis* STK 01

References	E_{24}
Amodu et al. (2014)	20%
This study	**50%**

The biosurfactant produced by *Bacillus licheniformis* STK 01 exclusively on *B.vulgaris* was identified as an effective emulsifier for a variety of hydrocarbons except for kerosene (Amodu et al., 2014). As highlighted earlier, this study showed improved emulsification of kerosene from the results obtained by Amodu et al. (2014), using the same organism and fermenter. The biosurfactant decreased interfacial tension between the kerosene and water, forming a stable film of emulsions, as shown in Figure 4-24, with the aid of nanoparticles. The addition of Ca-based biocompatible nanoparticles increased the stability of the emulsion by forming a solid layer between the emulsions.

The nanoparticles and the amphiphilic nature of the biosurfactant cooperatively aided in the stability of the emulsions. The hydrophobic head of the biosurfactant got adsorbed on the surface of the nanoparticles, increasing hydrophilicity of the system. This was confirmed by the obtained stable emulsions (Figure 4-24). A similar phenomenon was previously described by Józefczak and Wlazło (2015), where positively charged surfactant head groups got adsorbed on the surface of hydrophilic magnetic nanoparticles, exposing hydrophobic tails. With the emulsification of kerosene reported by Amodu et al. (2014) found to be just 20% (Table 4.4), the results obtained in this study for biosurfactant production in *B. vulgaris* supplemented with Ca-based nanoparticles showed enhanced biosurfactant yields and improved activity. This findings can have impactful environmental applications

Figure 4-24: Emulsion of kerosene by biosurfactant produced by *Bacillus licheniformis* STK 01

4.2.4 Summary

The ability of *Bacillus licheniformis* STK 01 to utilise *B. vulgaris* as a sole carbon source was revealed by biochemical analysis of the bacterium using Vitek systems. The results showed the microorganism's ability to produce enzymes that enable the it to utilise complex carbohydrates found in agrowaste. Crystal Ca-based nanoparticles enhanced the production of biosurfactant by *Bacillus licheniformis* in *B. vulgaris*, exclusively. The Ca-based nanoparticles influenced the bacterium's growth rate and biosurfactant yield, and improved activity. Increased growth rate and biosurfactant yield were obtained in media containing the Ca-based nanoparticles under both aerobic and anaerobic conditions. The fermentation conditions were closely monitored and it was determined that the nanoparticles had no adverse impact on the conditions. Biosurfactant produced in fed-batch fermentation under aerobic conditions with Ca-based nanoparticles supplemented at a 7 h interval had the highest biosurfactant yields. The biosurfactant activity was assessed by the emulsification of kerosene hydrocarbon and found to have an emulsification index of 50%, which is an improvement on previously reported studies using the same fermenter, organism and hydrocarbon.

CHAPTER 5
CONCLUSIONS AND RECOMMENDATIONS

5.1 CONCLUSIONS

Biosurfactants have been successfully used as alternatives for chemical surfactants for environmental bioremediation. However, the production of these surfactants has been coupled with high costs and low yields. This study has focused on overcoming the above-mentioned limitations. Ca-based nanoparticles were successfully synthesised using a single pot, green synthesis method to enhance biosurfactant production with *B. vulgaris* agrowaste. The following were achieved:

- A one-pot completely green chemistry method for the synthesis of Ca-based nanoparticles using *B. vulgaris* plant extract.
- Spherical-shaped crystal Ca-based nanoparticles (size of ≈10 nm) were synthesised from a 1% (v/v) *B. vulgaris* juice extract solution.
- Elevated temperatures and alkaline pH were determined to influence bio-reduction of metals facilitated by betanin to promote the subsequent synthesis of nanoparticles.
- *Aloe vera* was determined to be a useful reducing and capping agent in the green synthesis of nanoparticles for which large quantities of $CaCO_3$ solution from eggshells can be used to adjust the solution pH.
- The morphology of the nanoparticles can be modified by varying the *B. vulgaris* juice extract concentration.
- Ca^{2+} ion was more susceptible to reduction into Ca-based nanoparticles owing to its electrochemical potential and its high concentration in *B. Vulgaris* tubers.
- Characterisation using TEM and SEM-EDS confirmed the nano size and spherical morphology of the Ca-based nanoparticles.
- The UV-vis spectrum showed maximum absorbance of the Ca-based nanoparticles at 418 nm.
- Powder X-ray diffraction at an angle of 2 theta degrees illustrated characteristic of calcium line indexed at (001) and (100) with diffraction angles of 18.0 and 28.6 respectively.
- Betanin successfully capped the nanoparticles within a supporting matrix to prevent agglomeration during synthesis.
- Nanoparticle colloidal solution showed no sign of precipitation after being kept for two months, which indicated stability of the Ca-based nanoparticles.
- Biocompatibility of nanoparticles was confirmed by promoting *Bacillus licheniformis* STK01's growth, with higher growth rate being achieved in media containing the Ca-based nanoparticles under both aerobic and anaerobic conditions.

- 50% *B. vulgaris* solution with 50% Ca-based nanoparticle colloidal solution resulted in equal biosurfactant yield under both aerobic and anaerobic conditions.
- Biosurfactant production in fed-batch fermentation supplemented with nanoparticles at a 7 h interval under aerobic conditions had the highest yield of biosurfactant and improved emulsification activity.
- Ca-based nanoparticles had no adverse impact on dissolved oxygen utilisation, pH and redox potential by the bacterium.

The findings of this research provide an alternative route for single-pot, green synthesis of nanoparticles with the ability to facilitate large-scale production of biosurfactant in which agrowaste can be used as feedstock for STK 01. The improved activity of the biosurfactant can be employed for bioremediation of hydrophobic contaminants in the environment.

5.2 RECOMMENDATIONS

The following recommendations are suggested for future research:

- Consider measures to control environmental parameters such as pH and mV.
- Determine biological means to control foaming in the system.
- Study biosurfactant production kinetics.
- Prior to environmental applications of the biosurfactant, characterisation of the biosurfactant extract makeup be optimised to further increase activity

REFERENCES

Amodu, O.S., Ntwampe, S.K.O. & Ojumu, T.V. 2014. Optimization of biosurfactant production by *Bacillus licheniformis* STK 01 grown exclusively on *Beta vulgaris* waste using response surface methodology. *BioResources*, 9(3):5045-5065.

Anand, B., Sudha, S., Keshaw, A. & Harit, J. 2013. Value added products from agrowaste. *Recent Research in Science & Technology*, 5(2):7-12.

Anwar, Z., Gulfraz, M. & Irshad, M. 2014. Agro-industrial lignocellulosic biomass a key to unlock the future bio-energy: a brief review. *Journal of Radiation Research and Applied Sciences*, 7(2):163-173.

Attia, Gamila Y., Moussa, M.E.M. & Sheashea, E.R. 2013. Characterization of red pigment extracted from red beet (*Beta vulgaris,* L.) and its potential uses as antioxidant and natural food colorants. *Egyptian Journal of Agricultural Research*, 91(3):1095-1110.

Banat, I.M. 1995. Biosurfactants production and possible uses in microbial enhanced oil recovery and oil pollution remediation: a review. *Bioresource Technology*, 51(1):1-12.

Banat, I.M., Satpute, S.K., Cameotra, S.S., Patil, R. & Nyayanit, N.V. 2014. Cost effective technologies and renewable substrates for biosurfactants' production. *Frontiers in Microbiology*, 5(Art. 697):1-18.

Bhardwaj, G., Cameotra, S.S. & Chopra, H.K. 2015. Utilization of oil industry residues for the production of rhamnolipids by *Pseudomonas indica*. *Journal of Surfactants and Detergents*, 18(5):887-893.

Bhatia, L., Johri, S. & Ahmad, R. 2012. An economic and ecological perspective of ethanol production from renewable agro waste: a review. *Applied Microbiology and Biotechnology Express*, 2(1):65.

Burgos-Díaz, C., Piqué, C.N., Manresa Presas, M. & & Marqués Villavecchia, A.M. 2012. Advances in the research of new biosurfactants and their potential use in the biomedical and pharmaceutical industry. In Muñoz-Torrero, D., Haro, D. & Vallès, J. (eds). *Recent advances in pharmaceutical sciences II.* Kerala, India: Transworld Research Network: 151-167.

Camilios-Neto, D., Bugay, C., De Santana-Filho, A.P., Joslin, T., De Souza, L.M., Sassaki, G.L., Mitchell, D.A. & Krieger, N. 2011. Production of rhamnolipids in solid-state cultivation using a mixture of sugarcane bagasse and corn bran supplemented with glycerol and soybean oil. *Applied Microbiology and Biotechnology*, 89(5):1395-1403.

Clarridge, J.E. 2004. Impact of 16S rRNA gene sequence analysis for identification of bacteria on clinical microbiology and infectious diseases. *Clinical Microbiology Reviews*, 17(4):840-862.

Clontz, L. 2009. *Microbial limit and bioburden tests: validation approaches and global requirements*. 2nd ed. Boca Raton, FL: CRC Press.

Coronel-León, J., De Grau, G., Grau-Campistany, A., Farfan, M., Rabanal, F., Manresa, A. & Marqués, A.M. 2015. Erratum to: Biosurfactant production by AL 1.1, a *Bacillus licheniformis* strain isolated from Antarctica: production, chemical characterization and properties. *Annals of Microbiology*, 65(4):2065-2079.

Dadrasnia, A. & Ismail, S. 2015. Biosurfactant production by *Bacillus salmalaya* for lubricating oil solubilization and biodegradation. *International Journal of Environmental Research and Public Health*, 12(8):9848-9863.

Darroudi, M., Bagherpour, M., Hosseini, H.A. & Ebrahimi, M. 2016. Biopolymer-assisted green synthesis and characterization of calcium hydroxide nanoparticles. *Ceramics International*, 42(3): 3816-3819.

Das, P., Mukherjee, S. & Sen, R. 2008. Genetic regulations of the biosynthesis of microbial surfactants: an overview. *Biotechnology and Genetic Engineering Reviews*, 25(1):165-186.

De Azeredo, H.M.C., Pereira, A.C., De Souza, A.C.R., Gouveia, S.T & Mendes, K.C.B. 2009. Study on efficiency of betacyanin extraction from red beetroots. *International Journal of Food Science & Technology*, 44(12):2464-2469.

De Boer, A.S., Priest, F. & Diderichsen, B. 1994. On the industrial use of *Bacillus licheniformis*: a review. *Applied Microbiology and Biotechnology*, 40(5):595-598.

Desai, J.D. & Banat I.M. 1997. Microbial production of surfactants and their commercial potential. *Microbiology and Molecular Biology Reviews*. 61(1): 47-64.

Dewaliya, V. & Jasodani, R. 2012. Isolation and identification of soil isolates of *Pseudomonas* species via FAME analysis. *International Journal of Scientific Research*, 2(9):360-361.

Divakaran, D., Chandran, A. & Pratap Chandran, R. 2011. Comparative study on production of α-Amylase from *Bacillus licheniformis* strains. *Brazilian Journal of Microbiology*, 42(4):1397-1404.

DWAF (Department of Water Affairs and Forestry). 1998. Minimum requirements for waste disposal by landfill. 2nd ed. Pretoria: Department of Water Affairs and Forestry.

Eddouaouda, K., Mnif, S., Badis, A., Younes, S.B., Cherif, S., Ferhat, S., Mhiri, N., Chamkha, M. & Sayadi, S. 2012. Characterization of a novel biosurfactant produced by *Staphylococcus* sp. strain 1E with potential application on hydrocarbon bioremediation. *Journal of Basic Microbiology*, 52(4):408-418.

Farias, C.B.B., Silva, A.F., Rufino, R.D., Luna, J.M., Souza, J.E.G. & Sarubbo, L.A. 2014. Synthesis of silver nanoparticles using a biosurfactant produced in low-cost medium as stabilizing agent. *Electronic Journal of Biotechnology*, 17(3):122-125.

Farn, R.J. 2006. *Chemistry and technology of surfactants*. Oxford: Blackwell.

Flores, M., Colón, N., Rivera, O., Villalba, N., Baez, Y., Quispitupa, D., Avalos, J. & Perales, O. 2004. A study of the growth curves of *C. xerosis* and *E. coli* bacteria in mediums containing cobalt ferrite nanoparticles. *Materials Research Society Proceedings,* 820:8-17.

Fracchia, L., Cavallo, M., Martinotti, M. & Banat, I. 2012. Biosurfactants and bioemulsifiers biomedical and related applications – present status and future potentials. In Ghista, D.N. (ed.). *Biomedical science, engineering and technology*. Rijeka, Croatia: InTech: 325-370. http://cdn.intechopen.com/pdfs-wm/26371.pdf [25 May 2016].

Franzetti, A., Gandolfi, I., Bestetti, G., Smyth, T.J.P. & Banat, I.M. 2010. Production and applications of trehalose lipid biosurfactants. *European Journal of Lipid Science and Technology*, 112(6):617-627.

Fritze, D. 2004. Taxonomy of the genus *Bacillus* and related genera: the aerobic endospore-forming bacteria. *Phytopathology*, 94(11):1245-1248.

Gan, P.P., Ng, S.H., Huang, Y. & Li, S.F. 2012. Green synthesis of gold nanoparticles using palm oil mill effluent (POME): A low-cost and eco-friendly viable approach. *Bioresource Technology*, 113:132-135.

Ghribi, D. & Ellouze-Chaabouni, S. 2011. Enhancement of *Bacillus subtilis* lipopeptide biosurfactants production through optimization of medium composition and adequate control of aeration. *Biotechnology Research International*, 2011:1-6.

Grangemard, I., Bonmatin, J.M., Bernillon, J., Das, B.C. & Peypoux, F. 1999. Lichenysins G, a novel family of lipopeptide biosurfactants from *Bacillus licheniformis* IM 1307: production, isolation and structural evaluation by NMR and mass spectrometry. *Journal of Antibiotics,* 52(4):363-373.

Gudiña, E.J., Fernandes, E.C., Rodrigues, A.I., Teixeira, J.A. & Rodrigues, L.R. 2015. Biosurfactant production by *Bacillus subtilis* using corn steep liquor as culture medium. *Frontiers in Microbiology*, 6(Art. 59):1-7. doi:10.3389/fmicb.2015.00059.

Hanauer, M., Pierrat, S., Zins, I., Lotz, A. & Sönnichsen, C. 2007. Separation of nanoparticles by gel electrophoresis according to size and shape. *Nano Letters*, 7(9): 2881-2885.

Herrera, J.E. & Sakulchaicharoen, N. 2009. Microscopic and spectroscopic characterization of nanoparticles. In Pathak, Y. & Thassu, D. (eds). *Drug delivery nanoparticles: formulation and characterization, vol. 2.* New York, NY: Informa Healthcare: 237-251.

Hommel, R.K. 1990. Formation and physiological role of biosurfactants produced by hydrocarbon-utilizing microorganisms. Biosurfactants in hydro carbon utilization. *Biodegradation*, 1(2-3):107-119.

Ismail, W., Alhamad, N.A., El-Sayed, W.S., El Nayal, A.M., Chiang, Y.R. & Hamzah, R.Y. 2013. Bacterial degradation of the saturate fraction of Arabian light crude oil: biosurfactant production and the effect of ZnO nanoparticles. *Journal of Petroleum & Environmental Biotechnology*, 4:163. doi:10.4172/2157-7463.1000163.

Joshi, S.J., Geetha, S.J. & Desai, A.J. 2015. Characterization and application of biosurfactant produced by *Bacillus licheniformis* R2. *Applied Biochemistry and Biotechnology*, 177(2): 346-361.

Joshi, S.J., Suthar, H., Yadav, A.K., Hingurao, K. & Nerurkar, A. 2013. Occurrence of biosurfactant producing *Bacillus* spp. in diverse habitats. *International Scholarly Research Notices Biotechnology*, 2013(Art. 653240):1-6.

Józefczak, R. & Wlazło, R. 2015. Ultrasonic studies of emulsification stability in the presence of magnetic nanoparticles. *Advances in Condensed Matter Physics*, 2015(Art. 3984219):1-9.

Kalimuthu, K., Suresh Babu, R., Venkataraman, D., Bilal, M. & Gurunathan, S. 2008. Biosynthesis of silver nanocrystals by *Bacillus licheniformis*. *Colloids and Surfaces B: Biointerfaces*, 65(1):150-153.

Kalska-Szostko, B., Rogowska, M., Dubis, A.T. & Szymański, K. 2012. Enzymes immobilization on Fe_3O_4-gold nanoparticles. *Applied Surface Science*, 258(7):2783-2787.

Kiran, G.S., Nishanth, L.A., Priyadharshini, S., Anitha, K. & Selvin, J. 2014. Effect of Fe nanoparticle on growth and glycolipid biosurfactant production under solid state culture by marine *Nocardiopsis* sp. MSA13A. *BioMedCentral Biotechnology*, 14(48):1-10.

Kiran, G.S., Selvin, J., Manilal, A. & Sujith, S. 2011. Biosurfactants as green stabilizers for the biological synthesis of nanoparticles. *Critical Reviews in Biotechnology*, 31(4):354-364.

Konz, D., Doekel, S. & Marahiel, M.A. 1999. Molecular and biochemical characterization of the protein template controlling biosynthesis of the lipopeptide lichensysin. *Journal of Bacteriology*, 181(1):133-140.

Kowalczyk, B., Lagzi, I. & Grzybowski, B.A. 2011. Nanoseparations: strategies for size and/or shape-selective purification of nanoparticles. *Current Opinion in Colloid &*

Interface Science, 16(2):135-148.

Kuppusamy, P., Yusoff, M.M., Maniam, G.P. & Govindan, N. 2014. Biosynthesis of metallic nanoparticles using plant derivatives and their new avenues in pharmacological applications: an updated report. *Saudi Pharmaceutical Journal*. (In press, corrected proof).

Le, V.H., Thuc, C.N.H. & Thuc, H.H. 2013. Synthesis of silica nanoparticles from Vietnamese rice husk by sol–gel method. *Nanoscale Research Letters*, 8(Art.58):1-10.

Lee, S.W., Chang, S.H., Lai, Y.S., Lin, C.C., Tsai, C.M., Lee, Y.C., Chen, J.C. & Huang, C.L. 2014. Effect of temperature on the growth of silver nanoparticles using plasmon-mediated method under the irradiation of green LEDs. *Materials*, 7(12):7781-7798.

Link, S. & El-Sayed, M.A. 2000. Shape and size dependence of radiative, non-radiative and photothermal properties of gold nanocrystals. *International Reviews in Physical Chemistry*, 19(3):409-453.

Liu, J., Vipulanandan, C., Cooper, T.F. & Vipulanandan, G. 2013. Effects of Fe nanoparticles on bacterial growth and biosurfactant production. *Journal of Nanoparticle Research*, 15(Art.1405):1-13.

Luz Martínez, S., Romero, R., López, J.C., Romero, A., Sánchez Mendieta, V. & Natividad, R. 2011. Preparation and characterization of CaO nanoparticles/NaX zeolite catalysts for the transesterification of sunflower oil. *Industrial & Engineering Chemistry Research*, 50(5):2665-2670.

Maddikeri, G.L., Gogate, P.R. & Pandit, A.B. 2015. Improved synthesis of sophorolipids from waste cooking oil using fed batch approach in the presence of ultrasound. *Chemical Engineering Journal*, 263:479-487.

Makarov, V.V., Makarova, S.S., Love, A.J., Sinitsyna, O.V., Dudnik, A.O., Yaminsky, I.V., Taliansky, M.E. & Kalinina, N.O. 2014. Biosynthesis of stable Iron oxide nanoparticles in aqueous extracts of *Hordeum vulgare* and *Rumex acetosa* plants. *Langmuir*, 30(20):5982-5988.

Makkar, R. & Cameotra, S. 2002. An update on the use of unconventional substrates for biosurfactant production and their new applications. *Applied Microbiology and Biotechnology*, 58(4):428-434.

Maqsood, M.I & Jamal, A. 2011. Factors affecting the rhamnolipid biosurfactant production. *Pakistan Journal of Biotechnology*. 8(1):1-5.

Marchant, R. & Banat, I.M. 2012. Biosurfactants: a sustainable replacement for chemical surfactants? *Biotechnology Letters*, 34(9):1597-1605.

Maughan, H. & Van der Auwera, G. 2011. *Bacillus* taxonomy in the genomic era finds phenotypes to be essential though often misleading. *Infection, Genetics and Evolution*, 11(5):789-797.

Miller, G.L. 1959. Use of dinitrosalicylic acid reagent for determination of reducing sugar.

Analytical Chemistry, 31(3):426-428.

Mitchell, D.A. & Von Meien, O.F. 2000. Mathematical modeling as a tool to investigate the design and operation of the zymotis packed-bed bioreactor for solid-state fermentation. *Biotechnology and Bioengineering*, 68(2):127-135.

Mitchell, D.A., Krieger, N. & Berovic, M. 2006. *Solid-state fermentation bioreactors: fundamentals of design and operation*. Berlin: Springer.

Mubayi, A., Chatterji, S., Rai, P.M. & Watal, G. 2012. Evidence based green synthesis of nanoparticles. *Advanced Materials Letters*, 3(6):519-525.

Mulligan, C.N., Yong, R.N. & Gibbs, B.F. 2001. Surfactant-enhanced remediation of contaminated soil: a review. *Engineering Geology*, 60(1-4):371-380.

Murakami, F.S., Rodrigues, P.O., De Campos, C.M.T. & Silva, M.A.S. 2007. Physicochemical study of $CaCO_3$ from egg shells. *Ciência e Tecnologia de Alimentos*, 27(3):658-662.

Mussatto, S.I. & Teixeira, J.A. 2010. Lignocellulose as raw material in fermentation processes. In Méndez-Vilas, A. (ed.). *Current research, technology and education topics in applied microbiology and microbial biotechnology*. Badajoz, Spain: Formatex Research Center: 897-907.

Neagu, C. & Barbu, V. 2014. Principal component analysis of the factors involved in the extraction of beetroot betalains. *Journal of Agroalimentary Processes and Technologies*, 20(4):311-318.

Nerurkar, A.S. 2010. Structural and molecular characteristics of lichenysin and its relationship with surface activity. *Advances in Experimental Medicine and Biology*, 672:304-315.

Nitschke, M., Ferraz, C. & Pastore, G.M. 2004. Selection of microorganisms for biosurfactant production using agroindustrial wastes. *Brazilian Journal of Microbiology*, 35(1-2):81-85.

Nkosi, N.P. 2014. Waste tyre management trends and batch pyrolysis feasibility studies in Gauteng, South Africa. Unpublished MTech: Chemical Engineering dissertation, University of Johannesburg, South Africa.

Parameshwaran, R., Kalaiselvam, S. & Jayavel, R. 2013. Green synthesis of silver nanoparticles using *Beta vulgaris*: role of process conditions on size distribution and surface structure. *Materials Chemistry and Physics*, 140(1):135-147.

Płaza, G.A., Chojniak, J. & Banat, I.M. 2014. Biosurfactant mediated biosynthesis of selected metallic nanoparticles. *International Journal of Molecular Sciences*, 15(8):13720-13737.

Pohlscheidt, M., Charaniya, S., Bork, C., Jenzsch, M., Noetzel, T.L. & Luebbert, A. 2013. Process and fermentation monitoring. In Flickinger, M.C. (ed.). *Encyclopedia of industrial biotechnology: bioprocess, bioseparation and cell technology.* Hoboken, NJ: John Wiley: 1469-1491.

Prabu, R., Kuila, A., Ravishankar, R., Rao, P.V.C., Choudary, N.V. & Velankar, H.R. 2015. Microbial rhamnolipid production in wheat straw hydrolysate supplemented with basic salts. *Royal Society of Chemistry Advances*, 5(64):51642-51649.

Price, L.B., Liu, C.M., Melendez, J.H., Frankel, Y.M., Engelthaler, D., Aziz, M., Bowers, J., Rattray, R., Ravel, J., Kingsley, C., Keim, P.S., Lazarus, G.S. & Zenilman, J.M. 2009. Community analysis of chronic wound bacteria using 16S rRNA gene-based pyrosequencing: impact of diabetes and antibiotics on chronic wound microbiota. *PLoS One*, 4(7):e6462.

Rangarajan, V. & Sen, R. 2013. An inexpensive strategy for facilitated recovery of metals and fermentation products by foam fractionation process. *Colloids and Surfaces B: Biointerfaces*, 104:99-106.

Rangarajan, V. & Sen, R. 2013. An inexpensive strategy for facilitated recovery of metals and fermentation products by foam fractionation process. *Colloids and Surfaces B: Biointerfaces*, 104:99-106.

Reis, R.S., Pacheco, G.J., Pereira, A.G. & Freire, D.M.G. 2013. Biosurfactants: production and applications. In Chamy, R. & Rosenkranz, F. (eds). *Biodegradation – life of science.* Rijeka, Croatia: Intech: 31-61.

Reshmi, S.K., Aravindhan, K.M. & Devi, P.S. 2012. The effect of light, temperature, pH on stability of betacyanin pigments in *Basella alba* fruit. *Asian Journal of Pharmaceutical and Clinical Research*, 5(4):107-110.

Rey, M.W., Ramaiya, P., Nelson, B.A., Brody-Karpin, S.D., Zaretsky, E.J., Tang, M., Lopez de Leon, A., Xiang, H., Gusti, V., Clausen, I.G., Olsen, P.B., Rasmussen, M.D., Andersen, J.T., Jørgensen, P.L., Larsen, T.S., Sorokin, A., Bolotin, A., Lapidus, A., Galleron, N., Ehrlich, S.D. & Berka, R.M. 2004. Complete genome sequence of the industrial bacterium *Bacillus licheniformis* and comparisons with closely related *Bacillu*s species. *Genome Biology*, 5(10): ArtR77.

Roongsawang, N., Washio, K. & Morikawa, M. 2010. Diversity of non-ribosomal peptide synthetases involved in the biosynthesis of lipopeptide biosurfactants. *International Journal of Molecular Sciences*, 12(1):141-172.

Safaei-Ghomi, J., Ghasemzadeh, M.A. & Mehrabi, M. 2013. Calcium oxide nanoparticles catalyzed one-step multicomponent synthesis of highly substituted pyridines in aqueous ethanol media. *Scientia Iranica*, 20(3):549-554.

Saharan, B.S., Sahu, R.K. & Sharma, D. 2012. A review on biosurfactants: fermentation, current developments and perspectives. *Genetic Engineering and Biotechnology Journal*, 2011(Art.29):1-10.

Saini, J.K., Saini, R. & Tewari, L. 2015. Lignocellulosic agriculture wastes as biomass feedstocks for second-generation bioethanol production: concepts and recent developments. *3Biotech*, 5(4):337-353.

Sekhon, K.K., Khanna, S. & Cameotra, S.S. 2011. Enhanced biosurfactant production through cloning of three genes and role of esterase in biosurfactant release. *Microbial Cell Factories*, 10(Art.49):1-10.

Shyamala, Jr., B.N. & Jamuna, P. 2010. Nutritional content and antioxidant properties of pulp waste from *Daucus carota* and *Beta vulgaris*. *Malaysian Journal of Nutrition*, 16(3):397-408.

Singh, B. & Hathan, B.S. 2014. Chemical composition, functional properties and processing of beetroot – a review. *International Journal of Scientific and Engineering Research,* 5(1):679-684.

Slepecky, R.A. & Hemphill, H.E. 2006. The genus *Bacillus* – nonmedical. *Prokaryotes*, 4:530-562

Soberón-Chávez, G. (ed.). 2011. *Biosurfactants: from genes to applications*. Heidelberg: Springer.

Taglieri, G., Mondelli, C., Daniele, V., Pusceddu, E. & Trapanati, A. 2013. Synthesis and X-ray diffraction analysis of calcium hydroxide nanoparticles in aqueous suspension. *Advances in Materials Physics and Chemistry*, 3:108-112.

Thaniyavarn, J., Roongsawang, N., Kameyama, T., Haruki, M., Imanaka, T., Morikawa, M. & Kanaya, S. 2003. Production and characterization of biosurfactants from *Bacillus licheniformis* F2.2. *Bioscience, Biotechnology and Biochemistry*, 67(6):1239-1244.

University of Essex. 2014. Measurement techniques for nanoparticles. Colchester: University of Essex for NanoCap. http://www.nanocap.eu/Flex/Site/Downloadf860.pdf [25 May 2016].

Usman, M.S., Ibrahim, N.A., Shameli, K., Zainuddin, N. & Yunus, W.M.Z.W. 2012. Copper

nanoparticles mediated by chitosan: synthesis and characterization via chemical methods. *Molecules*, 17(12):14928-14936.

Van Bogaert, I.N.A., Saerens, K., De Muynck, C., Develter, D., Soetaert, W. & Vandamme, E.J. 2007. Microbial production and application of sophorolipids. *Applied Microbiology and Biotechnology*, 76(1):23-24.

Van Dyk, J.S., Sakka, M., Sakka, K. & Pletschke, B.I. 2009. The cellulolytic and hemi-cellulolytic system of *Bacillus licheniformis* SVD1 and the evidence for production of a large multi-enzyme complex. *Enzyme and Microbial Technology*, 45(5):372-378.

Vanaja, M. & Annadurai, G. 2012. *Coleus aromaticus* leaf extract mediated synthesis of silver nanoparticles and its bactericidal activity. *Applied Nanoscience*, 3(3):217-223.

Vanaja, M., Rajeshkumar, S., Paulkumar, K., Gnanajobitha, G., Malarkodi, C. & Annadurai, G. 2013. Kinetic study on green synthesis of silver nanoparticles using *Coleus aromaticus* leaf extract. *Advances in Applied Science Research*, 4(3):50-55.

Varadavenkatesan, T. & Murty, V.R. 2013. Production of a lipopeptide biosurfactant by a novel *Bacillus* sp. and its applicability to enhanced oil recovery. *International Scholarly Research Notices Microbiology*, 2013(Art. 621519):1-8.

Vecino Bello, X.V., Devesa-Rey, R., Cruz, J.M. & Moldes, A.B. 2012. Study of the synergistic effects of salinity, pH, and temperature on the surface-active properties of biosurfactants produced by *Lactobacillus pentosus*. *Journal of Agricultural and Food Chemistry*, 60(5): 1258-1265.

Veith, B., Herzberg, C., Steckel, S., Feesche, J., Maurer, K.H., Ehrenreich, P., Bäumer, S., Henne, A., Liesegang, H., Merkl, R., Ehrenreich, A. & Gottschalk, G. 2004. The complete genome sequence of *Bacillus licheniformis* DSM13, an organism with great industrial potential. *Journal of Molecular Microbiology and Biotechnology*, 7(4): 204-211.

Vijayalakshmi, S., Ranjitha, J. & Devi Rajeswari, V. 2013. Enzyme production ability by *Bacillus subtilis* and *Bacillus licheniformis: a* comparative study. *Asian Journal of Pharmaceutical and Clinical Research*, 6(4):29-32.

Vogel, H.C. & Todaro, C.L. 1997. *Fermentation and biochemical engineering handbook: principles, process design, and equipment*. 2nd ed. Westwood, NJ: Noyes.

Wadekar, S., Kale, S., Lali, A., Bhowmick, D. & Pratap, A. 2011. Sophorolipid production by *Starmerella bombicola* (ATCC 22214) from virgin and waste frying oils, and the effects of activated earth treatment of the waste oils. *Journal of the American Oil Chemists' Society*, 89(6):1029-1039.

White, D.A., Hird, L.C. & Ali, S.T. 2013. Production and characterization of a trehalolipid biosurfactant produced by the novel marine bacterium *Rhodococcus* sp. strain PML026. *Journal of Applied Microbiology*, 115(3):744-755.

Wuana, R.A. & Okieimen, F.E. 2011. Heavy metals in contaminated soils: a review of sources, chemistry, risks and best available strategies for remediation. *International Scholarly Research Notices Ecology*, 2011(Art. 402647):1-20.

Wybraniec, S. & Michałowski, T. 2011. New pathways of betanidin and betanin enzymatic oxidation. *Journal of Agricultural and Food Chemistry*, 59(17):9612-9622.

Yakimov, M.M., Kröger, A., Slepak, T.N., Giuliano, L., Timmis, K.N. & Golyshin, P.N. 1998. A putative lichenysin A synthetase operon in *Bacillus licheniformis*: initial characterization. *Biochimica et Biophysica Acta (BBA). Gene Structure and Expression*, 1399(2-3):141-153.

Yangtse, W., Zhou, Y., Lei, Y., Qiu, Y., Wei, X., Ji, Z., Qi, G., Yong, Y., Chen, L. & Chen, S. 2012. Genome sequence of *Bacillus licheniformis* WX-02. *Journal of Bacteriology*, 194(13):3561-3562.

Yu, M., Liu, Z., Zeng, G., Zhong, H., Liu, Y., Jiang, Y., Li, M., He, X. & He, Y. 2015. Characteristics of mannosylerythritol lipids and their environmental potential. *Carbohydrate Research*, 407:63-72.

Yu, M., Liu, Z., Zeng, G., Zhong, H., Liu, Y., Jiang, Y., Li, M., He, X. and He, Y. 2015. Characteristics of mannosylerythritol lipids and their environmental potential. *Carbohydrate Research*, 407:63-72.

Zhao, F., Shi, R., Zhao, J., Li, G., Bai, X., Han, S. & Zhang, Y. 2014. Heterologous production of *Pseudomonas aeruginosa* rhamnolipid under anaerobic conditions for microbial enhanced oil recovery. *Journal of Applied Microbiology*, 118(2):379-389.

APPENDICES

APPENDIX A: Analytical procedures

A1. Calibrating solutions chemical composition

A1.1 TISAB

58.4 g of sodium chloride, 61.50 g of sodium acetate, 0.29 g of sodium citrate and 15 ml of acetic acid in 1000 ml of distilled water.

A1.2 Anoxic solution

0.1M solution of sodium ascorbate and sodium hydroxide.

APPENDIX B: Determination of reducing sugars

B1. Reagents

B1.1. DNS solution

3,5-Dinitrosalicylic acid (DNS) reagent. Dissolve 10 g dinitrosalycylic acid, 2 g phenol, 0.5 g sodium sulphite and 10 g sodium hydroxide in 1 L distilled water.

B1.2. 40% potassium sodium tartrate

Dissolve 40 g of potassium sodium tartrate in 1 L of distilled water.

B2. The glucose standard curve

Standard solutions used to construct a g calibration curve were prepared according to Miller (1959). A stock solution containing 1000 mg/L of glucose was prepared and a series of standard solutions was prepared by diluting the stock solution to 100, 200, 300, 400, 500, 600, 700 and 1000 mg/L.

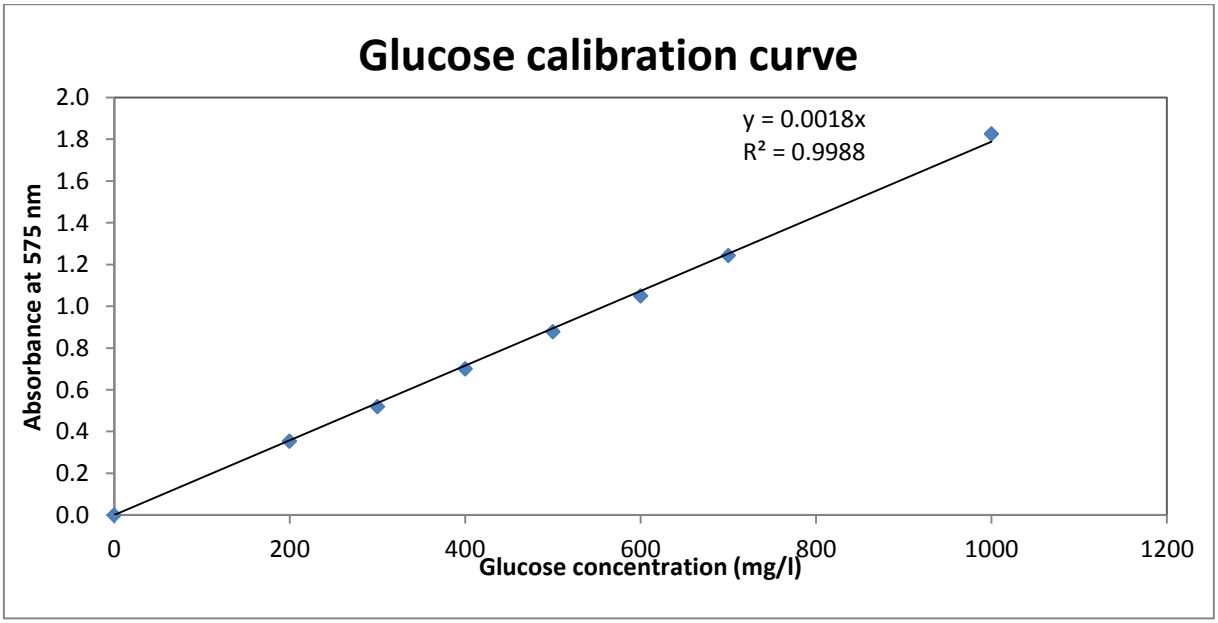

Figure 0-1: Calibration curve using DNS method

B2.1 Calculation of reducing sugar concentration

The reducing sugar concentration in the samples was calculated from the standard curve,

Sugar concentration (X) = $\frac{Y\ (Abs)}{0.0018}$

APPENDIX C: EDS spectrum results

C1. EDS spectrum of Sample 3

Owner: supervisor

Site: Site of Interest

3

Sample: Sample 2 19 Nov.

Type: Default

ID:

Sample 3

Processing option: All elements analysed (normalised)

All results in weight %

Spectrum	In stats.	C	O	Si	S	Ca	Total
Spectrum 1	Yes	21.19	62.46	0.8	0.23	15.32	100

Spectrum 2	Yes	36.41	52.5	1.2	0.61	9.28	100
Spectrum 3	Yes	51.68	39.89	1.22	1.3	5.9	100
Mean		36.43	51.62	1.07	0.71	10.17	100
Std deviation		15.25	11.31	0.24	0.54	4.77	
Max.		51.68	62.46	1.22	1.3	15.32	
Min.		21.19	39.89	0.8	0.23	5.9	

C2.EDS spectrum for Sample 7

Project: Carol

CPUT

Owner:

Supervisor

Site: Site of Interest 2

Sample: Sample 7 19 Nov.

Type: Default

ID:

Processing option: All elements analysed (normalised)

All results in weight %

Spectrum	In stats.	C	O	Al	Si	Total
Spectrum 1	Yes	39.54	45.04	14.21	1.21	100
Spectrum 2	Yes	32.22	49.84	16.56	1.38	100
Spectrum 3	Yes	26.68	52.33	19.81	1.19	100
Mean		32.81	49.07	16.86	1.26	100
Std deviation		6.45	3.7	2.81	0.11	
Max		39.54	52.33	19.81	1.38	
Min		26.68	45.04	14.21	1.19	